Earth-Science Reviews 155 (2016) 28–48

Contents lists available at ScienceDirect

Earth-Science Reviews

journal homepage: www.elsevier.com/locate/earscirev

Magnetic mineral assemblages in soils and paleosols as the basis for paleoprecipitation proxies: A review of magnetic methods and challenges

Daniel P. Maxbauer [a,b,*], Joshua M. Feinberg [a,b], David L. Fox [a]

[a] Department of Earth Sciences, University of Minnesota, Minneapolis, MN, United States
[b] Institute for Rock Magnetism, University of Minnesota, Minneapolis, MN, United States

ARTICLE INFO

Article history:
Received 10 August 2015
Received in revised form 11 January 2016
Accepted 26 January 2016
Available online 27 January 2016

Keywords:
Paleoprecipitation
Proxy
Soil magnetism
Paleosols
Iron oxides
Environmental magnetism

ABSTRACT

Magnetic iron oxide minerals, principally magnetite, maghemite, hematite, and goethite are formed in well-drained soils in response to a suite of physical, chemical, and biological factors. Despite a wide range of complexity in the pedogenic processes that lead to magnetic mineral formation, dissolution, and transformation, there are well-documented empirical relationships between various magnetic mineral assemblages in soils with environmental and climatic conditions. Recently there has been an increase in the number of quantitative magnetic paleoprecipitation proxies that have been developed, and there is great potential for magnetic methods to be used in the geologic record to develop reconstructions of past climates. Magnetic paleoprecipitation proxies have been widely utilized in Quaternary or younger loess–paleosol systems; however, they have yet to be utilized in the pre-Quaternary fossil record. Future studies of magnetic mineralogy of soils and paleosols should aim to explore non-loessic modern soils and pre-Quaternary paleosols with more focus on understanding the interaction between magnetic mineral assemblages and soil moisture. Applications of existing and novel magnetic paleoprecipitation proxies in the fossil record should prove to be a valuable resource for paleoclimatologists.

Contents

* Corresponding author at: 310 Pillsbury Drive SE, Minneapolis, MN 55455, United States.
E-mail address: maxba001@umn.edu (D.P. Maxbauer).

http://dx.doi.org/10.1016/j.earscirev.2016.01.014
0012-8252/

1. Introduction

Magnetism in well-drained soil is controlled by the abundance, grain size, and chemical composition of various iron oxide and oxyhydroxide minerals (hereafter referred to simply as 'oxides'). In soils, the most abundant (by volume) iron oxides are goethite (α-FeOOH) and hematite (α-Fe_2O_3), which are antiferromagnetic and produce weak permanent magnetizations. Magnetite (Fe_3O_4) and maghemite (γ-Fe_2O_3), both ferrimagnetic with strong magnetizations, are far less abundant in soils but tend to dominate bulk magnetic properties. Magnetic minerals form in soil in response to a suite of complex pedogenic processes that are sensitive to physical, chemical, and biological conditions. Despite these complexities, empirical relationships between soil iron oxides and climate have been observed for decades (e.g., Kampf and Schwertmann, 1983) and environmental magnetic studies of soils and sediments routinely make qualitative climatic interpretations (see reviews by Maher, 1998, 2007, 2011; Liu et al., 2012).

Quantitative reconstructions of past environmental conditions, such as mean annual precipitation and temperature, are of fundamental interest to paleoclimatologists. For example, methods to reconstruct paleoprecipitation in pre-Quaternary terrestrial systems (>2.6 Ma) have been developed using leaf physiognomic approaches (Peppe et al., 2011; Royer, 2012), bulk geochemical weathering indices of paleosols (Sheldon et al., 2002; Sheldon and Tabor, 2009), the depth to the carbonate horizon of paleosols (Retallack, 2005), and the ecophysiology of mammalian fauna (e.g., Eronen et al., 2010a; Eronen et al., 2010b). A growing number of studies have proposed methods to link magnetic minerals within a soil quantitatively to the mean annual precipitation (MAP) under which the soil developed (e.g., Maher and Thompson, 1995; Geiss et al., 2008; Balsam et al., 2011; Orgeira et al., 2011; Hyland et al., 2015). Historically this work has focused on magnetite/maghemite variations in loess-derived soils developed under a limited range of MAP (~200–1000 mm yr^{-1}), although some recent studies have expanded their scope to recognize quantitative relationships between precipitation rates and the abundance of hematite and goethite in soils that have experienced more rainfall (up to 3000 mm yr^{-1}; Long et al., 2011; Hyland et al., 2015).

Magnetic paleoprecipitation proxies have the potential to be broadly applicable to pre-Quaternary paleosols. However, current models have large uncertainties (Heslop and Roberts, 2013; Maher and Possolo, 2013) and it is clear from well-studied loess–paleosol sequences in China (Maher and Thompson, 1991; Porter et al., 2001), New Zealand (Ma et al., 2013), Alaska (Begét et al., 1990), North America (Geiss et al., 2004; Geiss and Zanner, 2006, 2007), and Russia (Maher et al., 2002; Maher et al., 2003a) that relationships between iron oxide mineralogy and MAP can vary regionally. This variability highlights the need to re-evaluate our current understanding of the factors that control the abundance of iron oxides in soils, the magnetic methods we use to identify them, and the potential applicability of magnetic paleoprecipitation proxies to paleosols in the pre-Quaternary geological record.

In the first part of this review we provide an overview of the major iron oxide minerals found in soils (Section 2). This is followed by a discussion of the pedogenic processes that lead to the formation and transformation of magnetic iron oxides in soils (Section 3). We then discuss the relevant magnetic methods used to identify and quantify the abundance of magnetic minerals in soils (Section 4). The available magnetic paleoprecipitation proxies are reviewed in Section 5. In Section 6 we address natural mechanisms that complicate and limit the applicability of different magnetic paleoprecipitation proxies. Further, we explore the potential pathways for iron oxide mineral destruction or transformation due to diagenetic processes that occur during the transition from soil to paleosol (Section 7). We conclude this review with a number of challenges and research themes that we hope will guide future research (Section 8).

We direct readers that are relatively new to the field of environmental magnetism to the appendix (Appendix A) where we include a brief primer on many common magnetic properties. This review draws from a broad body of previously published work. For further details on specific topics, readers are referred to the following resources: for a full review of iron oxide minerals see Cornell and Schwertmann (2003); for previous reviews on magnetism in soils see Mullins (1977) and Maher (1998); for more encompassing reviews of environmental magnetism in general see Thompson and Oldfield (1986), Evans and Heller (2003), Maher (2007), Maher (2011), and Liu et al. (2012).

2. Major iron oxides in soil

We describe here the magnetic minerals that display correlation between mineral abundance and precipitation (i.e., goethite, hematite, magnetite, maghemite). In addition, we have included some related information about ferrihydrite because it is a common soil constituent and often is involved as a precursor phase in pedogenic processes that lead to the formation of the more stable magnetic iron oxides. Lepidocrite (γ-FeOOH) is a polymorph of goethite that is generally less abundant compared with other iron oxides, but is associated with goethite in some poorly drained redoximorphic soils (Schwertmann, 1988; Till et al., 2014). Siderite ($FeCO_3$), greigite (Fe_3S_4), and pyrrhotite (Fe_7S_8–$Fe_{11}F_{12}$) are other magnetic iron minerals that are sometimes found in poorly drained, water-logged soils (Postma, 1983; Fassbinder and Stanjek, 1994). The hydration state of these water-logged soils is often more related to drainage than to climate, and the production of these minerals is not necessarily related to precipitation in most cases.

2.1. Magnetite and maghemite

Magnetite (Fe_3O_4) is a mixed Fe(II)/Fe(III) oxide with an inverse spinel crystal structure (see Fig. 1). Ferric iron occupies all of the tetrahedral A-sites (yellow in Fig. 1) while both Fe(III) and Fe(II) occupy octahedral B-sites (maroon in Fig. 1). The spin moments of A-site and B-site iron atoms are aligned antiparallel along the crystallographic 111 axis (denoted <111> in Fig. 1) and the imbalance caused by Fe(II)

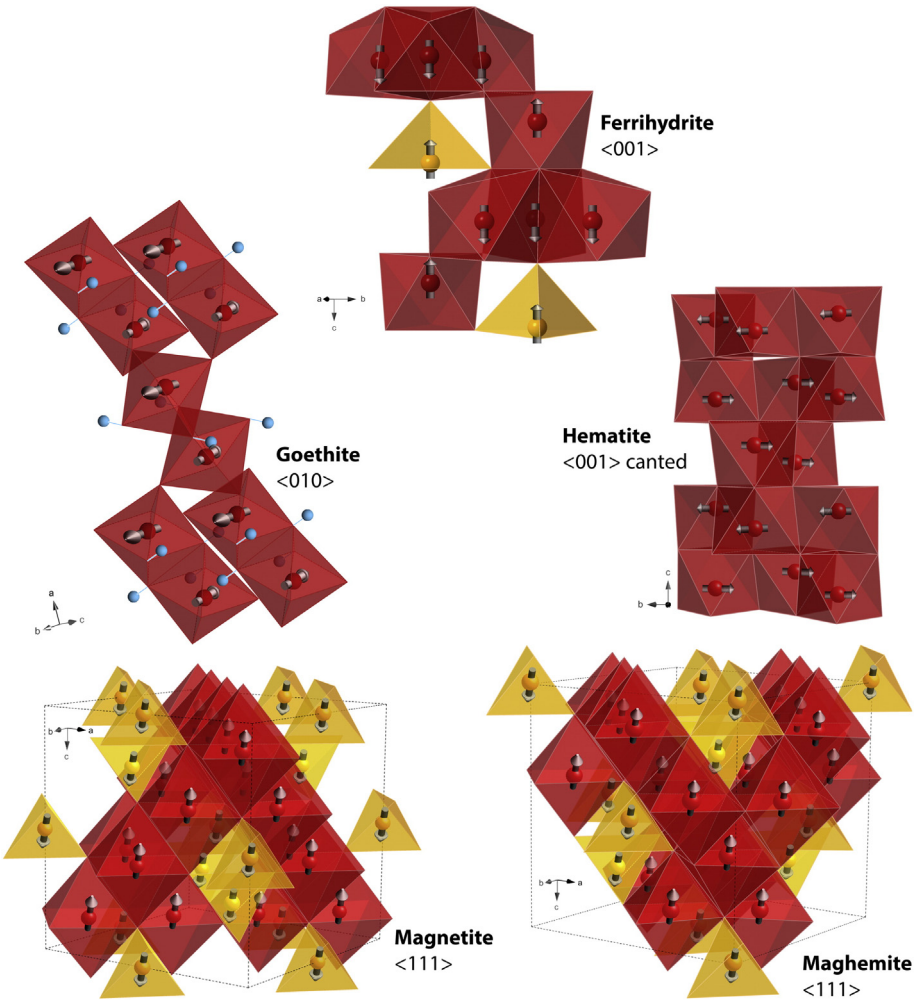

Fig. 1. Crystal structure and magnetic moment alignments for common soil iron oxides and hydroxides. Orientations of the magnetic moments for individual iron atoms are shown with gray arrows. Octahedral sites are shown in maroon and tetrahedral sites are shown in yellow. Hydrogen is shown as blue in the crystal structure of goethite. In each mineral structure the alignment of individual spin moments of iron atoms are aligned antiparallel along the indicated crystallographic axes. Except in the case of hematite, shown here with hexagonal crystal structure, where the spin alignment is nearly anti-parallel within the c-plane (above 260 K) however because of spin-canting of neighboring iron atoms there is a weak permanent magnetization that aligns along to the c-axis (Stacey and Banerjee, 1974; Dunlop and Özdemir, 2001; Dunlop and Özdemir, 2006). For goethite, spin alignments are antiparallel along the b-axis and weak parasitic and permanent remanence is due to defects and substitutions within the crystal structure that are not shown here (Liu et al., 2006). In magnetite imbalance in the antiparallel alignment along the crystallographic <111> axis is due to Fe(II), which occupies octahedral B-sites, and gives rise to magnetite's ferromagnetic properties (Banerjee and Moskowitz, 1985). Maghemite is composed entirely of Fe(III) and its ferrimagnetism is attributed to cation vacancies within the B sub-lattice. Crystal structure and spin alignment for ferrihydrite follows Michel et al. (2010). Note that the spin alignment for ferrihydrite shown here represents the transient ferrimagnetic ferrihydrite (also referred to as "hydromaghemite") phase that has been identified as a possible source of magnetic enhancement in soils. See Section 5.1.2 for more discussion. (For interpretation of the references to color in this figure legend, the reader is referred to the web version of this article.)

within the B sub-lattice gives rise to magnetite's ferrimagnetism (Banerjee and Moskowitz, 1985). Maghemite (γ-Fe_2O_3) is a ferric oxide with similar cubic spinel crystal structure and ferrimagnetic properties to magnetite. The ferrimagnetism of maghemite is due to vacancies within octahedral B-sites that cause imbalance between the A and B sub-lattice alignment along the <111> axis (Fig. 1).

Magnetite and maghemite are typically minor constituents (by volume or mass) of both bulk soils and the magnetic mineral fraction, but their ferrimagnetic properties tend to dominate many of the magnetic properties of soils (Maher, 1998). Magnetic susceptibility (χ; defined in Section A.1) values for magnetite can be as high as ~500 × 10^{-6} m^3kg^{-1}, with slightly lower values for maghemite (Maher, 2007). Saturation magnetization ($\boldsymbol{M_s}$; see Section A.3) for magnetite is ~92 A m^2 kg^{-1} and ~74 A m^2 kg^{-1} for maghemite (Pauthenet, 1950; Hunt et al., 1995; Tauxe et al., 2014). For an assemblage of purely stable single domain (SSD) magnetite/maghemite grains with random orientations a saturation remanence ($\boldsymbol{M_{rs}}$; see Section A.3) would be half of $\boldsymbol{M_s}$ ($\boldsymbol{M_{rs}}/\boldsymbol{M_s}$ = 0.5; Day et al., 1977; Parry, 1982; Dunlop, 2002). This ratio decreases both as grain size increases into multi domain (MD) size classes and/or as grain size decreases and behavior begins to resemble that of superparamagnetic (SP) grains (see Section A.2 for further discussion of magnetic grain size). Coercivity ($\boldsymbol{B_c}$) and coercivity of remanence ($\boldsymbol{B_{cr}}$) for magnetite and maghemite are generally low (typically 10s of mT; parameters defined in Section A.3) with a maximum $\boldsymbol{B_{cr}}$ for magnetite of ~300 mT (Hunt et al., 1995), meaning that saturation properties of these minerals can be easily studied using instruments that are standard to most rock magnetic laboratories. Magnetite and maghemite are referred to as magnetically "soft" minerals because of their relatively low coercivities.

2.2. Hematite and goethite

Hematite (α-Fe_2O_3) and goethite (α-FeOOH) are both so-called 'antiferromagnetic' minerals and are usually the most abundant and stable iron oxides present in the soil environment (Cornell and Schwertmann, 2003). Despite their nearly antiferromagnetic alignments both hematite and goethite produce weak permanent magnetizations (note that pure antiferromagnetism is characterized by a lack of

permanent magnetization in the absence of an applied field). In hematite, weak permanent magnetization arises at temperatures above ~260 K (temperature of the Morin transition in hematite) due to spin canting in neighboring iron atoms that have magnetic moments nearly antiparallel within the crystallographic c-plane (see Fig. 1; Stacey and Banerjee, 1974; Dunlop and Özdemir, 2001; Dunlop and Özdemir, 2006). When temperature falls below the Morin transition (~260 K) the spin alignment in pure hematite will become perfectly antiparallel along the c-axis and the weak permanent magnetization due to canting is lost (Stacey and Banerjee, 1974). In goethite, a weak permanent magnetization is due to parasitic remanence that arises as a result of defects and substitutions within the crystal structure (Fig. 1; Liu et al., 2006). In general, hematite and goethite are best characterized by their relatively weak magnetizations and remarkably high coercivities (see below).

The χ of hematite and goethite is similar, and roughly 2–3 orders of magnitude weaker than ferrimagnetic minerals (Dekkers, 1989; Maher, 2007). The saturation magnetization and remanence (M_s and M_{rs}) of these minerals is less well-constrained, but typically reported values for M_s are ~0.4 A m^2 kg^{-1} for pure hematite and ~0.05–0.30 A m^2 kg^{-1} for naturally occurring goethite (Dekkers, 1989; Maher, 2007; Martin-Hernandez and García-Hernández, 2010; Martin-Hernandez and Guerrero-Suárez, 2012; Özdemir and Dunlop, 2014). The M_{rs}/M_s ratio in goethite and hematite is typically between 0.5 and 1 and is sensitive to variations in grain size and degree of saturation (for example, calculating the ratio for goethite, for which true saturation is often not possible to achieve, using magnetizations measured at 5 T vs. 9 T will likely yield variable results). Many previous studies report M_{rs}/M_s ratios that are largely incorrect, as they were calculated from non-saturated specimens (see Rochette and Fillion, 1989; Özdemir and Dunlop, 2014).

In contrast to the "soft" ferrimagnetic minerals, hematite and goethite are referred to as "hard" magnetic minerals due to their characteristically high B_{cr} (in general > 300 mT) and the large fields required to saturate these minerals. Maher et al. (2004) reported non-saturation in a range of hematite samples above 2 T and in some samples as high as ~4–5 T (achieving only ~60–70% true M_{rs} value at 2 T; Maher, 2011). In goethite, and some fine-grained hematite, non-saturation has been reported in fields up to 57 T, as an extreme example (Rochette et al., 2005). Goethite is almost never saturated in fields produced by most laboratory instruments (1–3 T) and some studies suggest that only 10–20% of the true M_{rs} is imparted by 2 T (e.g., Rochette and Fillion, 1989; France and Oldfield, 2000; Maher et al., 2004; Maher, 2011).

The magnetic properties of hematite and goethite can vary greatly depending on grain size, defect density, and crystalline impurities such as aluminum substitutions (e.g., Dekkers, 1989; Liu et al., 2004; Liu et al., 2006; Roberts et al., 2006; Özdemir and Dunlop, 2014). Goethite, which is prone to Al-substitution (Fitzpatrick, 1988), has a characteristic decrease in B_{cr} and an increase in M_s with increasing Al% (Liu et al., 2006; Roberts et al., 2006). Further, increasing Al% in goethite acts to lower the Néel temperature (400 K for pure goethite, above this temperature goethite is unable to hold stable remanence) towards room temperature (Liu et al., 2006; Roberts et al., 2006). Aluminum substitution in hematite results in an increase in B_{cr} and a more variable effect on M_s with increasing Al% (Liu et al., 2006; Roberts et al., 2006). These complications become important when using magnetic measurements to estimate the abundance of hematite and goethite in natural sediments (see Section 4.4).

2.3. Ferrihydrite

Ferrihydrite ($Fe_2O_3 \cdot 4H_2O$; Fig. 1) is a poorly crystalline, metastable ferric iron oxide that is ubiquitous in many modern soils, particularly in young soils where weathering rates are high (Childs, 1992; Schwertmann, 1993; Jambor and Dutrizac, 1998; Cornell and Schwertmann, 2003). Ferrihydrite occurs in small, nanoscale (1–7 nm) particles that typically form coatings on silt and sand sized soil particles. The small particle size and poor crystallinity of ferrihydrite result in a high specific surface area (200–500 m^2 g^{-1}) and a high residual structural charge, both of which act to make it highly reactive (Childs, 1992; Jambor and Dutrizac, 1998; Cornell and Schwertmann, 2003).

Ferrihydrite is a frequent precursor to the more thermodynamically stable iron oxides, such as goethite and hematite (see Cornell and Schwertmann, 2003). Despite its ubiquity, the magnetic properties of ferrihydrite are very poorly constrained. Further, the crystal structure of pure, synthetic ferrihydrite remains an active area of debate (e.g., Michel et al., 2007; Maillot et al., 2011; Manceau, 2012; Peak and Regier, 2012a, 2012b). Natural ferrihydrites are commonly impure (i.e., have isomorphic substitution) and sorb silica, aluminum, and soil organic matter (Cismasu et al., 2011; Cismasu et al., 2012; Cismasu et al., 2013). This results in a decrease in long-range crystallinity for natural ferrihydrites, as compared with synthetic samples, and causes spatially variable surface properties (e.g., Eusterhues et al., 2008; Cismasu et al., 2013). Accordingly, the crystal structure of natural ferrihydrite is even less well understood. Lab experiments that describe transformation pathways of iron oxides (discussed in more detail in Section 5) often use synthetic samples of 2-line or 6-line ferrihydrite (where the latter exhibits slightly more long range order than the former) or isolated natural specimens. The heterogeneity of natural ferrihydrites likely is a cause of the variable magnetic properties of ferrihydrite and of the complexities of transformation pathways that occur in soils.

3. Formation of iron oxides in soils

Iron oxide minerals occur in soils variously from pedogenic formation, input from eolian processes (i.e., wind-blown dust), formation by burning during forest and grassland fires, deposition from industrial pollution, or inheritance from the soil parent material. When using precipitation proxies that link soil iron oxides with climate processes, it is critical that the iron oxides of interest are formed through pedogenic processes related to the soil moisture budget, and ultimately the long term input of rainfall to the soil. Here, we focus solely on the *pedogenic* processes known to produce iron oxide minerals in soils.

In oxic soils with a pH greater than 3, dissolution of ferrous iron-bearing primary minerals (e.g., pyroxene, olivine, biotite, fayalite) releases Fe^{2+} ions into the soil solution where rapid oxidation occurs, and poorly soluble Fe^{3+} ions rapidly undergo hydrolysis to precipitate ferrihydrite (Schwertmann, 1988; Cornell and Schwertmann, 2003). Ferrihydrite is unstable with respect to the more crystalline ferrimagnetic and antiferromagnetic minerals and, with time, will progressively transform into these more stable phases as soil conditions allow.

3.1. Iron oxide formation models describing magnetic enhancement

In many well-drained soils there is an observed increase in χ (and certain other magnetic properties such as anhysteretic and isothermal remanent magnetization, ***ARM*** and ***IRM*** respectively; for descriptions of these parameters see Section A.3) between the upper A and/or B soil horizon compared to the unaltered parent material (e.g., Fig. 2). This phenomenon is referred to as "magnetic enhancement" and has been a topic of interest for decades (e.g., LeBorgne, 1955, 1960; Mullins, 1977; Dearing et al., 1996b; Maher, 1998; Boyle et al., 2010; Orgeira et al., 2011). Magnetic enhancement arises primarily from the presence of SP/SSD magnetite and/or maghemite. Below we discuss the two main pathways that are attributed to the pedogenic production of SP/SSD ferrimagnetic minerals in soils.

3.1.1. Redox oscillations and the fermentation mechanism

The first mechanism proposed to explain the magnetic enhancement of well drained, temperate soils involves a so called "fermentation" process in which redox oscillations during wet/dry cycles result

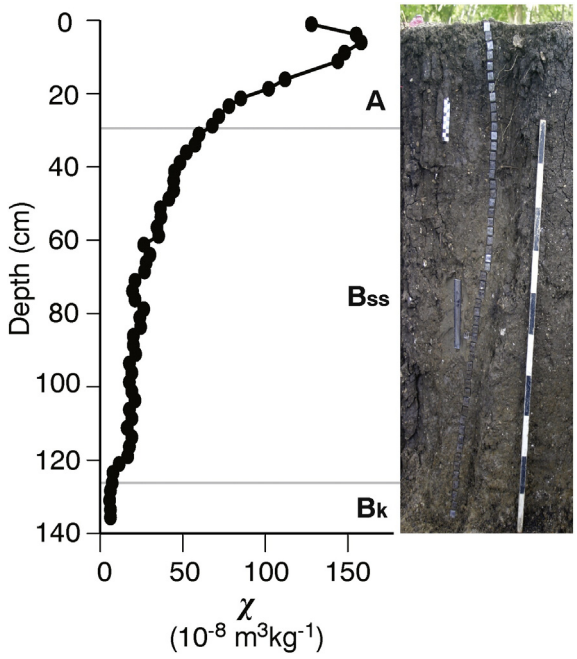

Fig. 2. Example of a magnetically enhanced alluvial Vertisol from Buttermilk Creek, Texas (Lindquist et al., 2011). Data at left is shown next to an image of the soil profile with sample cubes in place. The increase in magnetic susceptibility of the upper soil horizons relative to the lower horizons is common in many modern soils and is attributed in most cases to the pedogenic production of magnetite and/or maghemite. Magnetic unmixing methods have shown that "pedogenic" magnetite occurs in a variety of modern soils (see Fig. 3). Horizons are denoted with gray lines and follow descriptions in Lindquist et al. (2011). ss denotes presence of slickensides, k denotes the presences of carbonate. (For interpretation of the references to color in this figure, the reader is referred to the web version of this article.)

in the production of very-fine grained magnetite (LeBorgne, 1955, 1960; see reviews by Mullins, 1977; Maher, 1998; Orgeira et al., 2011). During wet periods, where water saturation in a soil is prolonged enough to create anoxic conditions in soil pore spaces, reduction of Fe (III) in oxides (primarily ferrihydrite) or other soil minerals releases Fe^{2+} into solution. The resultant mixed Fe^{2+}/Fe^{3+} solution can then precipitate nanocrystalline magnetite (in the SP/SSD size class) upon drying at near neutral pH (Taylor et al., 1987; Maher and Taylor, 1988).

This process has been demonstrated to occur abiotically in laboratory settings (Taylor et al., 1987; Maher and Taylor, 1988); however, under anoxic conditions the oxidation of organic matter is often coupled to the microbial reduction of Fe(III)-oxides in a process referred to as dissimilatory iron reduction (DIR; for reviews see Lovley et al., 2004; Lovley, 2013). The DIR bacterium *Geobacter metallireducins* (formerly strain GS-15) was the first organism discovered that coupled degradation of organic matter (acetate) to the reduction of ferric iron leading to the extracellular precipitation of SP/SSD magnetite (Lovley et al., 1987). This discovery was coincident with the experimental results of Taylor et al. (1987), which along with subsequent studies showed that biotic and abiotic precipitates of magnetite were both similar to natural SP/SSD magnetites (Maher and Taylor, 1988; Sparks et al., 1990). Despite a lack of direct observational evidence, it is now generally assumed that DIR bacteria play an integral role in the pedogenic production of magnetite during wet/dry cycles in well-drained temperate soils (e.g., Maher et al., 2003a; Guyodo et al., 2006; Maher, 2007).

Maghemite is commonly present in soils in combination with magnetite. The physical relationship between these two minerals is important to consider. Following the fermentation mechanism, maghemite is interpreted to have formed via the slow oxidation of magnetite (van Velzen and Dekkers, 1999; Chen et al., 2005; see Section 3.1.2 below for alternative model). The oxidation of magnetite occurs at the rims of individual grains and proceeds inward while oxidizing structural Fe^{2+} slowly diffuses out of the crystal structure. Oxidation of magnetite commonly results in partially oxidized magnetite grains that have a maghemitized rim and a magnetite core (van Velzen and Dekkers, 1999; Chen et al., 2005; Ge et al., 2014). Partial oxidation of magnetite may produce unusual, yet distinctive hysteresis behavior (e.g., Ge et al., 2014) and may ultimately lead to the complete maghemitization of the original grain.

3.1.2. Aging pathway of ferrihydrite to hematite

More recently, the slow transformation of ferrihydrite to hematite, during which an intermediate ferrimagnetic phase is produced, has been proposed as an alternative pathway that can lead to magnetic enhancement (Barron and Torrent, 2002; Barron et al., 2003; Torrent et al., 2006; Liu et al., 2008). Initial experiments showed that phosphate 2-line ferrihydrite ages to hematite in a two-step process where an ordered ferrimagnetic phase, similar to maghemite, is produced as a metastable intermediary (Barron and Torrent, 2002). Subsequent studies referred to the intermediate phase as hydromaghemite (Barron et al., 2003; Torrent et al., 2006; Liu et al., 2008; Cabello et al., 2009) and ferrimagnetic ferrihydrite (Michel et al., 2010; shown in Fig. 2). Extrapolation of laboratory conditions (transition occurs in the laboratory at ~150 °C under ambient atmosphere) indicates that the timescale for a full transformation of ferrihydrite to hematite would be on the order of 10^5–10^6 years. This transformation is highly dependent on the presence of ligands in the soil to effectively block the direct transformation of ferrihydrite to more thermodynamically favored phases, such as hematite and goethite, at such elevated temperatures (Liu et al., 2010).

Ferrihydrite is often categorized as one of two different types based on the number of distinctive X-ray diffraction peaks: 2-line and 6-line ferrihydrite. 2-line ferrihydrite is generally considered to represent a less crystalline form of ferrihydrite than 6-line. Aging of 2-line ferrihydrite at ~150 °C in open air results in the production of hematite with the characteristic magnetic intermediate phase being produced (Barron and Torrent, 2002). However, aging of 6-line ferrihydrite (~175 °C) undergoes a direct transformation to hematite or goethite without a magnetic intermediate phase (Barron et al., 2003). Tetrahedrally coordinated iron is thought to be present in 2-line, but not 6-line, ferrihydrite and maghemite (see Michel et al., 2007 and Janney et al., 2000), and this has been suggested as a reason why only 2-line ferrihydrite ages into a transient maghemite-like intermediary (Barron et al., 2003; Liu et al., 2010; see Fig. 1). However, recent work has reported the presence of tetrahedrally coordinated Fe(III) in 6-line ferrihydrite, which appears to have antiferromagnetic spin coupling between tetrahedral and octahedral sublattices (Guyodo et al., 2012). The crystallographic complexities in ferrihydrite highlight the likelihood that transformations of iron oxides in soils are more complex than controlled laboratory experiments.

An important gap in this aging model is that there is no pathway for the production of magnetite, which is a common pedogenic mineral that causes magnetic enhancement in modern soils. However, it does not appear to be necessary that these two pathways (fermentation and aging) be exclusive. There is no necessity for anoxic conditions in the ferrihydrite aging mechanism, so it may be the case that during prolonged dry seasons magnetic mineral production is associated primarily with ferrihydrite aging while rainy season conditions favor a fermentation model.

3.2. Goethite and hematite formation and distribution

Transformations of less crystalline iron oxides, like ferrihydrite, directly to goethite and hematite are common in soils and are dependent on the soil conditions. In general, goethite is favored in cool, moist soils that only rarely experience prolonged intervals of aridity. By contrast, hematite is more abundant in subtropical, Mediterranean, or tropical soils with frequent episodes of prolonged dryness (Kampf and Schwertmann, 1983; Schwertmann, 1988; Cornell and Schwertmann,

2003). Soils with near neutral pH and low organic content tend to favor hematite over goethite, and vice-versa (Schwertmann and Murad, 1983; Das et al., 2011).

Transformations between the more crystalline iron oxides are also possible, and likely occur in soils over a range of timescales. Goethite dehydroxylates to hematite when heated in ambient air in the laboratory and converts to magnetite when heating occurs in reductive conditions (Till et al., 2015). Hematite can also form simply as the ultimate product of the slow oxidation of magnetite (first to maghemite and then to hematite) via structural rearrangements (Cornell and Schwertmann, 2003). Transformations between iron oxides in soils after burial and disconnection with prevailing climatic conditions may be a serious source of error in any proxy method relating iron oxide minerals with precipitation, and this is discussed in more detail below. However, despite complexities in the transformational pathways described in laboratory experiments, the predominance of goethite and/or hematite in modern soils in specific environmental conditions suggests that climate does play a profound role in the iron mineralogy of soils (e.g., Kampf and Schwertmann, 1983).

4. Characterizing iron oxide mineral assemblages

Below we discuss the environmental magnetic parameters that have been utilized in previous work to characterize magnetic mineral assemblages with the aim of determining empirical relationships with precipitation. Some additional environmental magnetic methods and parameters are described in the appendix (Appendix A) and may be of interest to readers seeking further detail.

4.1. Frequency dependence of susceptibility

The frequency dependence of magnetic susceptibility (χ_{fd}) is a measure of the contribution of SP sized grains to the mass normalized magnetic susceptibility (χ, $m^3\ kg^{-1}$) of a specimen (Dearing et al., 1996a). Nearly all SP grains can become dynamically aligned with an alternating magnetic field (<~1×10^4 A m^{-1}) of low frequency (e.g., 465 Hz). The relaxation time of SP grains (τ, defined as the time for the magnetization of an ensemble of grains to decay to 1 / *e* of its original value following Nèel's equation; see Dunlop and Özdemir, 2001) is typically much shorter than the period of the weak alternating magnetic field (AF) used during measurement of susceptibility, and thus the magnetizations of these grains will contribute strongly to the measured magnetic susceptibility ($\chi_{465\ Hz}$; Thompson and Oldfield, 1986; Dearing et al., 1996a; Maher, 2007). However, at higher frequencies (e.g., 4650 Hz) the relaxation time of SP grains near the threshold for SP/SSD behavior is longer than the period of the AF. Accordingly, these grains are unable to fully align with the AF and their magnetization is out-of-phase with the alternating field. At such high frequencies these grains are no longer able to contribute as much to the measured magnetic susceptibility ($\chi_{4650\ Hz}$). Thus, specimens enriched in SP grains will display an inverse relationship between susceptibility and AF frequency. It is important to note that SSD and MD grains do not fully track the alternating current at either low or high frequency, and so their contribution to χ remains constant at variable frequency (Dearing et al., 1996a). Although we note, as an aside, that MD grains tend to show a variable χ response to the amplitude of the AF (Jackson et al., 1998).

It is conventional to report χ_{fd} as a percentage, where:

$$\chi_{fd} = [(\chi_{465\ Hz} - \chi_{4650\ Hz}) / \chi_{465\ Hz}] * 100. \quad (1)$$

Diamagnetic, paramagnetic, and non-saturated high-coercivity ferromagnetic minerals contribute equally to susceptibility regardless of frequency. Accordingly, the contribution of paramagnetic and diamagnetic minerals is removed from numerator, but not the denominator, when χ_{fd} is calculated according to Eq. (1). It is more appropriate to calculate the frequency dependence of susceptibility using the ferrimagnetic susceptibility (χ_{ferri}; defined in Section A.3) in the denominator (e.g., $\chi_{fd} = [(\chi_{465\ Hz} - \chi_{4650\ Hz}) / (\chi_{465\ Hz} - \chi_{ferri})] * 100$) so that the contribution of paramagnetic and diamagnetic minerals is removed in all cases. This is rarely done in practice and in many cases would only have a minimal impact on calculated values due to the low χ_{lf} values associated with diamagnetic and paramagnetic material. Although, we wish to emphasize the importance using χ_{ferri} in clay rich soils, where the contribution of paramagnetic minerals to susceptibility may be dominant (Dearing et al., 1996a; Yamazaki and Ioka, 1997; Jordanova and Jordanova, 1999).

The low and high frequency values of 465 Hz and 4650 Hz are not specific to the calculation of frequency dependence of magnetic susceptibility; nor is the specific form of Eq. (1), for example some researchers simply report the difference between the low and high frequency values, rather than normalize it (Thompson and Oldfield, 1986). These frequencies simply represent the factory settings included on the most commonly used commercial susceptibility meter in environmental magnetism labs around the world (the Bartington 2). However, regardless of the exact frequency values used, it is important to include instrument details, such as the frequency and amplitude of magnetic field, in published studies so that future workers may be able to reproduce the measurements.

In general, χ_{fd} percentages greater than ~6% indicate a considerable abundance of SP ferrimagnetic particles, while maximum observed values of ~15% indicate a specimen whose susceptibility is dominated by SP ferrimagnets (Dearing et al., 1996a). Studies of modern soils and loessic paleosols routinely use χ_{fd} as an indicator of SP ferrimagnets; although, this method cannot by itself distinguish the composition of the magnetic minerals in the specimen (e.g., magnetite vs. maghemite). However, magnetic paleoprecipitation proxies routinely use χ, χ_{fd}, and the susceptibility of ***ARM*** (χ_{ARM}; see Section A.3) as indirect measures of ferrimagnetic mineral abundance.

4.2. HIRM

The remanence held by "hard" magnetic minerals (goethite and hematite) within sediments has been estimated by the "hard" ***IRM***, or ***HIRM*** for decades (Robinson, 1986). ***HIRM*** is typically defined as half of the difference in saturation and non-saturation ***IRM*** (e.g., $\mathbf{HIRM} = 0.5 * \mathbf{SIRM} + \mathbf{IRM}_{-300\ mT}$; Robinson, 1986), where a backfield ***IRM*** (typically on the order of ~100–300 mT) is applied following saturation in the opposite direction. The origination of ***HIRM*** was based on the longstanding observation that above ~300 mT isothermal remanence is held primarily by hematite and/or goethite (Collinson, 1968). Increasing values of ***HIRM*** are interpreted to represent greater contributions of hard antiferromagnetic minerals to remanence.

Care needs to be taken in interpretations of soil ***HIRM*** for a number of reasons. First, ***HIRM*** is a remanence parameter, which means zero representation is given to SP grains and grains whose remanence state is a non-uniformly magnetized configuration will be underrepresented (e.g., pseudo-single domain, PSD, and multi-domain, MD, grains; see Section A.2). Second, ***HIRM*** is often calculated using "saturating" fields of ~1 T, which is too low to be a true saturating field for antiferromagnetic minerals (see Section 2.2 above). Finally, an implicit assumption in ***HIRM*** is that all antiferromagnetic minerals acquire only minimal remanence in fields < 300 mT, while the ferrimagnetic minerals stop acquiring additional remanence in fields > 300 mT (or some other intermediate field of choice). However, maghemite and partially oxidized magnetite can continue to acquire remanence in fields > 300 mT (Liu et al., 2002) and nanometer-scale or aluminous hematite can have widely variable $\mathbf{B_c}$ (Liu et al., 2007b; Özdemir and Dunlop, 2014). For these reasons, we stress that ***HIRM*** values be evaluated with some caution and that additional parameters be used to aid in the interpretation of ***HIRM*** data (e.g., Liu et al., 2002; see the appendix (Section A.4) for more detail).

4.3. Unmixing magnetic mineral components

Natural sediments represent a complex assemblage of magnetic minerals that vary in composition and magnetic grain size due to environmental or geological processes that promote iron oxide formation, dissolution, or transformation. In order to investigate these processes, it is often necessary to magnetically "unmix" sediments in order to identify the relative contributions from various individual magnetic mineral components (Robertson and France, 1994; Stockhausen, 1998; Kruiver et al., 2001; Heslop et al., 2002; Egli, 2003, 2004a, 2004b; Heslop et al., 2004; Geiss and Zanner, 2006; Heslop and Dillon, 2007; see Heslop, 2015 for a comprehensive and detailed review).

In the simplest sense, the intensity of remanence (***IRM*** or ***ARM***) is a reflection of remanence carried by SSD and MD grains. For example, take the following expressions for ***IRM*** and ***ARM*** (Geiss and Zanner, 2006):

$$IRM = IRM_{SSD} + IRM_{MD} = M_s \alpha_{ISD} f_{SSD} + M_s \alpha_{IMD}(1 - f_{SSD}) \quad (2)$$

$$ARM = ARM_{SSD} + ARM_{MD} = M_s \alpha_{ASD} f_{SSD} + M_s\, \alpha_{AMD}(1 - f_{SSD}) \quad (3)$$

where IRM_{SSD}, IRM_{MD} and their ***ARM*** equivalents are the SSD and MD components of ***IRM*** or ***ARM***, M_s is the saturation magnetization described in Section A.3, f_{SSD} is the volumetric fraction of SSD particles (ranging from 0 to 1), and the α terms describe the acquisition efficiency of SSD and MD domain grains for ***IRM*** (α_{ISD} and α_{IMD}) and ***ARM*** (α_{ASD} and α_{AMD}). The α terms are generally unknown but can be approximated based on theoretical and empirical arguments. Setting Eq. (2) equal to Eq. (3) yields a solvable expression for f_{SSD} that can be thought of as representing the "pedogenic" component of remanence (f_{ped}), because SSD magnetic minerals are often associated as byproducts of pedogenic processes (Section 3; Geiss and Zanner, 2006).

In many instances it is desirable to isolate the relative magnetic contribution of individual magnetic mineral phases (e.g., magnetite, hematite, etc.) within a specimen at a finer detail than simply SSD versus MD grains. Robertson and France (1994) proposed that because the shape of an ***IRM*** acquisition curve for a monomineralic specimen often resembles a cumulative log-Gaussian (CLG) function it may be possible to approximate a specimen's ***IRM*** acquisition curve given three parameters: the mean coercivity (B_h), a dispersion parameter (D_p, equivalent to one standard deviation in log space), and the inferred saturation ***IRM*** (M_r; see Fig. 3). If there is more than one magnetic mineral phase contributing to the measured ***IRM*** acquisition, Robertson and France (1994) suggested that each magnetic component could be represented by individual CLG functions where the parameters (B_h, D_p, and M_r) would be informative about their respective mineral phase.

If it assumed that any interaction between magnetic mineral grains is negligible, then a simple linear combination of these component CLG functions would create a modeled ***IRM*** acquisition curve that could be compared against observations (Robertson and France, 1994). Subsequent work built on these concepts and began to use log-Gaussian probability density functions to model coercivity spectra (the absolute value of the first derivative of a magnetization curve, e.g., ***IRM*** or ***ARM*** acquisition or demagnetization curves and backfield curves; see Fig. 3; Stockhausen, 1998; Kruiver et al., 2001; Heslop et al., 2002). Coercivity distributions represent the individual coercivities of all particles contained within a specimen. Models that approximate coercivity distributions for a natural specimen by linear combinations of component distributions assume that individual magnetic components represent a specific subset of magnetic minerals that are similar in composition, degree of crystallinity, grain size, grain shape, and concentration of defects (Egli, 2003).

Despite the wide use of log-Gaussian functions in modeling natural coercivity spectra, it was noted by Robertson and France (1994) and confirmed by subsequent studies (e.g., Egli, 2004b; Heslop et al., 2004) that many populations of magnetic mineral grains produce coercivity distributions that deviate from pure log-Gaussian behavior. The distribution of coercivities within a magnetic mineral assemblage can diverge from normality for a number of reasons, including: grain size distribution, grain elongation, thermal relaxation, and the initial magnetization state after demagnetization or saturation (see Egli, 2004b and Heslop et al., 2004 for details). Importantly, it appears that non-Gaussian behavior is to be expected in natural samples. In order to more accurately account for these deviations, Egli (2003) describes an adaption to the generalized Gaussian function (skewed generalized Gaussian, SGG) that incorporates both skewness and kurtosis. Many natural samples display left-skewed tails (particularly at low fields) that may require two log-Gaussian distributions to fit appropriately (Egli, 2004b; Heslop et al., 2004). In contrast, the SGG model of Egli (2003) allows for a single component to fit a skewed distribution. For this reason we suggest that methods incorporating skewness be favored over earlier work (Egli, 2003; Heslop et al., 2004; Heslop, 2015).

Unmixing methods have been applied to a wide range of natural materials, including soils (Egli, 2004a, b; Geiss et al., 2008; Lindquist et al., 2011). Importantly, the main parameters describing the distributions of individual magnetic components (B_h and D_p) are remarkably consistent for soils regardless of the unmixing methods used (see Fig. 3; Egli,

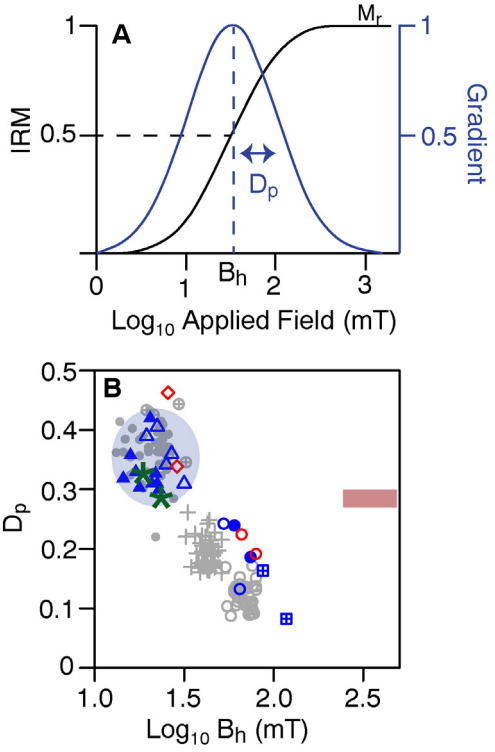

Fig. 3. A. Schematic representation of an ***IRM*** acquisition curve (in black) and its first derivative, commonly referred to as a coercivity distribution (in blue). The coercivity distribution can be described by its median coercivity (B_h) and the distribution width (dispersion parameter, D_p). Representation is a simplification of Fig. 1 from Kruiver et al. (2001) and assumes a log Gaussian probability distribution approximates the coercivity distribution. Note that both the IRM and Gradient data are normalized to their respective maximum values. B. A biplot of D_p and $\log_{10}$ (B_h) for isolated magnetic components from a mixture of natural sediments. Data taken from Egli (2004a), Geiss and Zanner (2006), and Lindquist et al. (2011). Blue shaded oval highlights the ranges of D_p and B_h observed for pedogenic magnetite in soils. Blue symbols = soils, gray symbols = lake sediments, red symbols = loess, green asterisks = dissimilatory iron reducing (DIR) bacteria produced magnetite (extracellular magnetite). Open triangles = detrital + pedogenic magnetite, closed triangles = pedogenic magnetite, open circles = biogenic hard component, open diamonds = eolian dust, + = biogenic soft magnetite, closed circles = detrital + extracellular magnetite. Red rectangle corresponds to the hematite component used by Abrajevitch et al. (2009). All magnetic component descriptions follow Egli (2004a). (For interpretation of the references to color in this figure legend, the reader is referred to the web version of this article.)

2004a; Geiss et al., 2008). In general, unmixing approaches are used in order to differentiate between various types of soft ferrimagnetic magnetite because field strengths achievable in most laboratories are sufficient to saturate the magnetization of these minerals (usually saturated in fields below ~300 mT). However, recent work has attempted to use the unmixing methods developed by Kruiver et al. (2001) to quantify the abundance of antiferromagnetic minerals in marine sediment cores (Abrajevitch et al., 2009) and soils (Hyland et al., 2015).

4.4. Determination of goethite and hematite concentrations

In order to effectively relate precipitation to the abundance of hematite and goethite within a soil it is critical that estimates of mineral abundances are accurate. Due to the large fields required to saturate both goethite and hematite, and their relatively weak magnetizations, it is common to estimate their absolute abundances using non-magnetic methods. The most commonly used techniques are X-Ray diffraction (XRD), diffuse reflectance spectroscopy (DRS; Balsam et al., 2004; Torrent et al., 2007; Zhang et al., 2007; Lyons et al., 2014; Hu et al., 2015), or Mössbauer spectroscopy (e.g., Carter-Stiglitz et al., 2006). Often these methods are more costly in comparison with magnetic approaches and are only sufficiently sensitive when the iron oxide minerals within a specimen are concentrated using chemical treatments (Liu et al., 2002). Magnetic determinations of hematite and goethite abundance would be advantageous because of their lower analytical costs, their greater sensitivity to iron oxides in low volume abundances, and for their potential to more quickly analyze a greater number of samples. However, despite the increasingly frequent use of magnetic methods (e.g., Sangode et al., 2008; Abrajevitch et al., 2009; Hao et al., 2009; Morón et al., 2013; Hyland et al., 2015) there is no straightforward protocol for accurately estimating the abundance of goethite or hematite by mass or volume from rock magnetic measurements (Hao et al., 2009).

One recent approach estimates the contribution of individual antiferromagnetic minerals to remanence by unmixing high field ***IRM*** acquisition curves (e.g., Abrajevitch et al., 2009; Hyland et al., 2015). This approach requires a priori knowledge of what magnetic minerals are present in a set of specimens (which, for example, can be achieved by the heating experiments described in the appendix, Section A.5) or an assumption that each of the magnetic components chosen to fit an ***IRM*** acquisition curve represents a different magnetic mineral. The M_{rs} value of each magnetic component in theory represents the M_{rs} held by an individual magnetic mineral (Kruiver et al., 2001). In order to convert these values into estimates of mass or volume, it is necessary to normalize the M_{rs} derived from unmixing with a M_{rs} value for a pure standard of hematite or goethite (e.g., Abrajevitch et al., 2009; Morón et al., 2013). There is considerable variability in the M_{rs} values for pure hematite and naturally occurring goethite (Fig. 4) due to grain size, crystal defects, substitutions, and the field strength used to achieve saturation (Dekkers, 1989; Liu et al., 2006; Özdemir and Dunlop, 2014). This is particularly true for goethite because of the extreme difficulty in achieving saturation (e.g., Rochette et al., 2005). We stress that care needs to be taken when magnetic measurements are converted into absolute estimates of mineral abundances by mass or volume.

5. Magnetic proxies for precipitation

In the mid 1980's researchers first began to recognize that variations in magnetic susceptibility of loess–paleosol sequences on the Chinese Loess Plateau (CLP) correlated well with marine $\delta^{18}O$ records of benthic foraminifera (Heller and Liu, 1986). This discovery sparked interest in using magnetic variations within loessic paleosol sequences to reconstruct climatic changes in central China. Early work aimed to elucidate the relative importance of various processes that might contribute to the observed magnetic variability. The two processes that received the most attention were aeolian dust flux, whose variability was controlled by regional monsoonal climate patterns, and pedogenic processes that intensified with increasing rainfall and temperature (e.g., Kukla et al., 1988; Maher and Thompson, 1991, 1992). Since these early studies there has been a tremendous amount of work on loess records in China (see recent review by Liu et al., 2007a) and elsewhere (Alaska, Russia, and Argentina) to explore the relationships between iron oxide mineralogy and climate. Here we focus only on the work that has documented correlation between precipitation and pedogenic magnetic minerals.

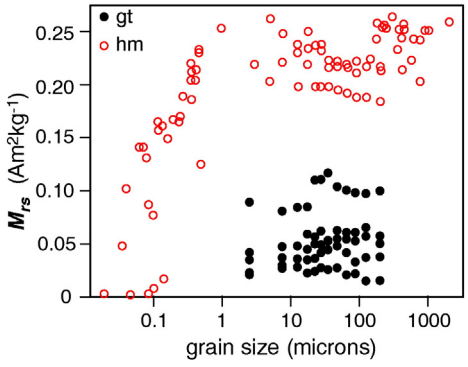

Fig. 4. Saturation remanence (M_{rs}) values reported in the literature for hematite (hm, shown in red) and goethite (gt, shown in black) shown with respect to grain size. Literature values displayed for hematite come from the compilation in Özdemir and Dunlop (2014) and for goethite are shown from Dekkers (1989). For goethite data, grain size ranges are reported in Dekkers (1989) and we plot data here according to the midpoint of each size class. Note that the M_{rs} values shown here are not necessarily true saturation values due to the large field required to saturate these minerals. The M_{rs} values for goethite were all acquired in a 15 T field (Dekkers, 1989). Field strengths corresponding to the reported values of M_{rs} in hematite vary. (For interpretation of the references to color in this figure legend, the reader is referred to the web version of this article.)

5.1. Relationships between magnetic enhancement and precipitation in loessic soils

After establishing that χ variations in CLP soils and paleosols were driven by the pedogenic production of SP/SSD magnetite (Maher and Thompson, 1991, 1992), quantitative estimates of the relationships between χ and mean annual precipitation (MAP; typically defined as a 30 year average of nearby or interpolated meteorological data) began to arise. Maher et al. (1994) introduced the concept of *pedogenic susceptibility* (χ_{ped}), which is an absolute measure of the difference in χ between a soil's B horizon and its underlying C horizon ($\chi_{ped} = \chi_B - \chi_C$; note that the C horizon is assumed to be equivalent to the parent material). The B horizon is used instead of the A horizon, which in most soils is more magnetically enhanced than the B horizon, in order to avoid the effects of contamination in modern soils and because the A horizon is rarely preserved in paleosols (Maher et al., 1994).

In a preliminary set of modern soils from the CLP (37 soils from 9 locations), χ_{ped} showed strong positive, log-linear correlation with MAP ($R^2 = 0.95$; Fig. 5) and was used to reconstruct precipitation records back some ~125 ka (Maher et al., 1994). Correlations between χ and mean annual temperature were also noted (Maher et al., 1994; Jiamao et al., 1996), although far more attention has been given to relationships with precipitation. Subsequent studies (e.g., Liu et al., 1995; Jiamao et al., 1996) observed similar empirical relationships between χ and climate on the CLP and recognized the potential for quantitative estimates of paleoprecipitation from magnetic mineral assemblages preserved within paleosols. The calibration of χ_{ped} with MAP was expanded to include loessic soils from across the Northern Hemisphere (Maher and Thompson, 1995), additional CLP soils (Porter et al., 2001), as well as loessic soils in Russia (Maher et al., 2002; Maher et al., 2003a).

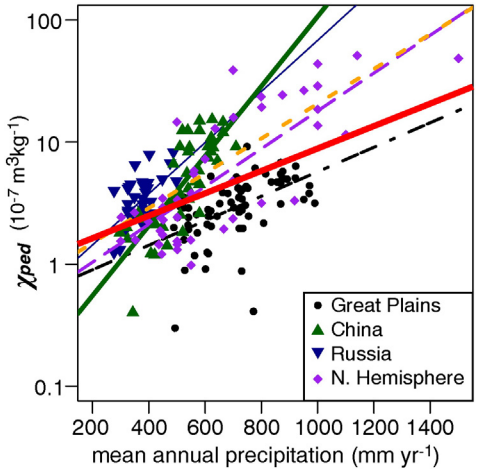

Fig. 5. Pedogenic susceptibility (χ_{ped}) versus mean annual precipitation. Great Plains data from Geiss et al. (2008) and Geiss and Zanner (2007), data for China are from Porter et al. (2001) and Maher et al. (1994), data from Russia from Maher et al. (2002) and Alekseev et al. (2003), and Northern Hemisphere data compiled in Maher and Thompson (1995). All lines represent simple linear regression models. All models were statistically significant ($p < 0.05$). Thin blue line = Russia ($R^2 = 0.35$), double dashed black line = Great Plains ($R^2 = 0.25$), thick green line = China ($R^2 = 0.61$), coarse-dashed purple line = N. Hemisphere ($R^2 = 0.60$), fine-dashed orange line = Russia, China, and N. Hemisphere data combined ($R^2 = 0.52$), thick solid red line = all data ($R^2 = 0.24$). (For interpretation of the references to color in this figure legend, the reader is referred to the web version of this article.)

However, the addition of more soils from diverse environmental settings introduced considerable scatter to the initial relationship ($n = 115$, $R^2 = 0.52$; see Fig. 5). More recent work on loessic soils in the U.S. Great Plains shows only weak positive correlation between χ_{ped} and MAP ($R^2 = 0.25$, $n = 72$; Geiss and Zanner, 2007; Fig. 5). A compilation of all available χ_{ped} data for loessic soils displays a similarly weak ($R^2 = 0.24$), but still significant ($p < 0.001$) positive correlation (see Fig. 9). Despite the statistical significance of these correlations, the relatively low R^2 values that result from combining regional datasets suggest that global χ_{ped} models are poor predictors of MAP.

Additional complications in the interpretation of soil magnetic mineral assemblages were revealed during investigations of loess–paleosol sequences in Alaska (Begét et al., 1990) and Argentina (Orgeira et al., 1998; Orgeira et al., 2003), which showed magnetic depletions in paleosols (in contrast to magnetic enhancement). In these settings the role of aeolian dust flux and wind strength was interpreted to outweigh the efficiency of pedogenic enhancement (Lagroix and Banerjee, 2002, 2004). Thus, it is important to note that no single model of soil magnetism can explain the magnetic mineral assemblage of all soils. Rather, the variability of local processes (e.g., wind speed, mean annual precipitation and temperature) can lead to different controlling mechanisms for the formation of magnetic minerals in soils, and great care needs to be taken during the interpretation of soil magnetism records.

The χ_{ped} parameter defined by Maher et al. (1994) is an example of an absolute magnetic enhancement parameter that aims to quantify the concentration of pedogenic magnetite and/or maghemite. Geiss and Zanner (2007) argue that simple ratios between magnetically enhanced soil horizons relative to their parent materials provide a more direct measure of pedogenic ferrimagnetic mineral production (e.g., χ_{enh}/χ_{parent}). Variations in the physical and chemical properties of the parent material can have a large influence on absolute enhancement parameters (see Section 6.1). For example, some geologic materials are enriched in iron (e.g., basalts), and thus, the absolute value of pedogenic enhancement for soils developed on these materials may be different than that of soils developed on less iron-rich materials (e.g., limestone). By using relative parameters, such as those proposed by Geiss and Zanner (2007), the influence of parent material is normalized. For the U.S. Great Plains, mean annual precipitation rates of loessic soils show stronger correlations with relative enhancement parameters (Geiss and Zanner, 2007; Geiss et al., 2008) than with absolute enhancement parameters like χ_{ped}. It is important to note, however, that despite these improved correlations with relative enhancement parameters, there are still regional differences in the relationships between precipitation and magnetic enhancement (Geiss and Zanner, 2007). Thus, a precipitation transform function calibrated using data from loessic soils in Russia is not able to accurately reproduce precipitation rates in the U.S. Great Plains. Extraneous variables such as the floral and faunal soil ecology or parent material (among others) are likely contributing to the observed regional variation in modern systems. The inability to sufficiently control for these variables in the fossil record poses a serious problem for the application of these methods to ancient systems.

In an effort to directly quantify magnetic enhancement and remove the influence of parent material altogether, Geiss et al. (2008) proposed the ratio of χ_{ARM}/IRM as a direct estimate of pedogenic (SSD) magnetite. For the loessic Great Plains soils, this ratio shows strong positive correlation with MAP ($R^2 = 0.70$; Fig. 6), although data from other areas again highlight regional differences (Geiss et al., 2008). Coercivity unmixing of modern soils has shown that the pedogenic magnetite component appears to be relatively consistent across different continents and environmental conditions (Egli, 2004a; Geiss and Zanner, 2006; Geiss et al., 2008). Typically, pedogenic magnetite/maghemite assemblages in modern soils have a B_h of ~20 mT and a D_p of ~0.3 ($\log_{10}$ scale; see shaded blue area in Fig. 3; Egli, 2004a; Geiss et al., 2008). Using coercivity unmixing to directly characterize the abundance of pedogenic magnetite in an individual specimen, rather than comparing an enhanced specimen to an unaltered parent material has major advantages over traditional approaches. If future work is able to describe pedogenic magnetite in more modern soils, across a range of soil types and climates, it may become possible to identify additional empirical relationships that exist solely between pedogenic magnetite and MAP or soil moisture. Ultimately, such approaches would render magnetic characterization of the parent material unnecessary (Geiss et al., 2008) but may prove challenging to develop.

A complicating factor in the relationship between MAP and magnetic enhancement in loessic soils is variation in soil moisture, which ultimately controls the chemical reactions that form or dissolve magnetic minerals in soil, that is not captured by changes in MAP (e.g., Porter et al., 2001; Orgeira et al., 2011). For example, in two systems receiving equivalent MAP but with different temperatures and vegetation there is

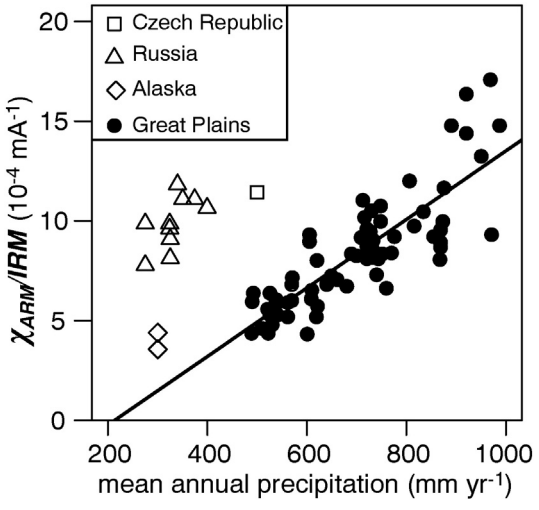

Fig. 6. Correlation between MAP and χ_{ARM}/IRM for an assemblage of modern loessic soils. Simple linear regression through the Great Plains data has an $R^2 = 0.70$ (data from Geiss et al., 2008). However, data from other locations highlight that regional variation exists in this relationship, which inhibits the predictive power of this relationship in ancient systems. Czech Republic data from Oches and Banerjee (1996), Russian data from Alekseev et al. (2003), and Alaska data from Sharpe (1996).

likely to be variation in soil moisture that will drive changes in the magnetic mineralogy. Orgeira et al. (2011) describe the *magnetic enhancement proxy* (MEP), which is a quantitative model based on physical principles that describes magnetic mineral production (magnetite and maghemite) with respect to soil moisture. The MEP model relates the soil moisture ratio (W), defined as the ratio of MAP to potential evapotranspiration (PET), with ferrimagnetic mineral production (p). The MEP model assumes that magnetite forms according to the fermentation mechanism (described in Section 3.1.1) where wet–dry cycles in soils are critical in maintaining the balance of ferrimagnetic mineral production and dissolution (see Orgeira et al., 2011 for details). Their model can more accurately describe variations in magnetic enhancement observed in loessic, and some non-loessic, soils from various geographical regions, which suggests that regional variations in the MAP magnetic enhancement correlations may be due more to deviations in soil moisture with respect to MAP than to variable regional processes that form magnetic minerals (Orgeira et al., 2011).

The MEP model successfully reproduces magnetic enhancements in many modern environments, although one of its limitations is that it relies on parameters that are difficult to extend to the past and that inhibit its use as a paleoenvironmental tool. The difficulty in applying the MEP model to ancient systems underscores the fact that many of our existing environmental magnetic tools for understanding past climate are based on overly simple variables that do not take into account natural processes that are known to influence the magnetic properties of modern soils. Future work should aim to develop new methods that incorporate aspects of the MEP, like the focus given to soil moisture, while remaining simple enough to allow for application to fossil systems.

All of the magnetic methods discussed to this point have been calibrated using modern soils, where magnetic enhancement is controlled by the pedogenic production of magnetite and/maghemite. MAP ranges for these calibrations are generally limited to temperate conditions between ~200–1000 mm yr^{-1}. Rates of pedogenesis are likely to be too slow to generate magnetic enhancement in climates where the MAP is less than 200 mm yr^{-1}. Conversely, in humid climates where MAP exceeds ~1000 mm yr^{-1}, it is observed that positive correlations between MAP and magnetic enhancement parameters either flatten (e.g., Maher and Thompson, 1995) or become negative (e.g., Balsam et al., 2011; Long et al., 2011). This non-linear response is attributed to the increased dissolution of iron oxides and leaching that persists in water-saturated soils with only limited dry periods (Maher, 2011). The calibration range for magnetic paleoprecipitation proxies poses an important problem in the fossil record where MAP exceeded ~1000 mm yr^{-1}. This problem is not unique to magnetic methods and also limits geochemically-based paleoprecipitation proxies for paleosols.

5.2. Relationships between precipitation and abundances of goethite and hematite

Goethite and hematite are more abundant (by volume and mass) in modern soils than magnetite and maghemite, and are also thought to be more stable and resistant to reductive dissolution. Further, as mentioned in Section 3.2, there is a well-documented, general relationship between goethite and hematite and climate, where hematite is generally thought to occur in warmer drier conditions, while goethite is thought to occur in cooler wetter environments (Kampf and Schwertmann, 1983). There have been a number of recent studies that have proposed precipitation proxies that include, either directly or indirectly, information about the abundance of goethite and hematite (Balsam et al., 2004; Torrent et al., 2007; Torrent et al., 2010b; Torrent et al., 2010a; Long et al., 2011; Liu et al., 2013; Hyland et al., 2015).

Qualitative interpretations of paleoprecipitation changes are often inferred using variable abundances of goethite with respect to hematite. For example, Balsam et al. (2004) used DRS-based estimates of goethite and hematite abundances to study climatic variations on the CLP dating back some 2.6 Ma. Sangode and Bloemendal (2004) used goethite-to-hematite ratios, estimated using $\boldsymbol{IRM_{4-3\,T}/IRM_{1-0.5\,T}}$ (where remanence acquired between fields of between 4 and 3 T is attributed to goethite and between 1 and 0.5 T is attributed to hematite), to reconstruct the soil hydration state of Pliocene-Pleistocene paleosols of the Siwalik Group from the Himalaya, India. Later studies from modern soils in Spain highlighted the relationship between hematite (derived from DRS) and χ_{fd} and suggested that precipitation reconstructions should be based on proxies such as the hematite-to-χ_{fd} ratio or a ratio of hematite to goethite (Torrent et al., 2007; Torrent et al., 2010b; Torrent et al., 2010a).

A promising study of 10 modern soils in China spanning ~300–1000 mm yr^{-1} MAP shows a strong, positive correlation with χ_{fd}/***HIRM*** of the A/B horizons ($R^2 = 0.92$; Liu et al., 2013). In theory, this relationship represents the partitioning of iron between hard magnetic phases such as goethite and hematite (as represented by ***HIRM***) and SP ferrimagnets (represented by χ_{fd}) during pedogenesis. Higher values correspond to a greater iron allocation to magnetite and/or maghemite as MAP increases up to ~1000 mm yr^{-1}. The χ_{fd}/***HIRM*** ratio is calculated as the slope of a bivariate plot of χ_{fd} versus ***HIRM*** (where the "background" values for each parameter are subtracted from the data) for the entire B horizon, which removes the need to construct an enhancement ratio or to select an "enhanced" sample from the B horizon alone (Liu et al., 2013).

Other recent studies have presented encouraging new magnetic paleoprecipitation proxies that relate MAP to the ratio of goethite-to-hematite (***Gt***/***Hm***) in modern soils distributed globally (Hyland et al., 2015) and for a climosequence in South China (Long et al., 2011). Methods relating ***Gt***/***Hm*** to MAP are particularly desirable because this ratio appears to be sensitive to a wide range of MAP (200–3000 mm yr^{-1}; Hyland et al., 2015) and goethite and hematite are likely to be stable iron oxide minerals over geologically relevant timescales. Hyland et al. (2015) report ***Gt***/***Hm*** ratios for the B horizon of 70 modern soils that have a remarkably strong correlation with MAP ($R^2 = 0.96$; Fig. 7). Long et al. (2011) also report a strong correlation between the ratio of hematite-to-goethite and MAP within soil B horizons ($R^2 = 0.64$; Layer II in Long et al., 2011 taken as equivalent to B horizon; Fig. 7). These new correlations demonstrate the great potential that ***Gt***/***Hm*** based magnetic paleoprecipitation proxies may hold for application in the fossil record.

Although ***Gt***/***Hm*** paleoprecipitation proxies hold considerable potential for advancing paleoclimate studies, we note a number of problems inherent in the analytical approach taken by Hyland et al. (2015). Hyland et al. (2015) assign mineral abundances to goethite and hematite using remanence unmixing methods developed by Kruiver et al. (2001). This approach is problematic for two reasons. First, minor amounts of cation substitution (usually Al) into goethite or hematite can dramatically alter the coercivities of these minerals (Liu et al., 2006; Roberts et al., 2006), and thus, the magnetic components identified using these proxies may not in fact accurately represent the true concentrations of goethite and hematite present in a specimen. Second, the proxies are only sensitive to a fraction of the goethite present in a specimen. Unusually high fields (as much as >57 T; Rochette et al., 2005) are required to fully saturate goethite, whereas most paleomagnetic labs are only able to generate impulse fields of ~5 T. Thus, the highest coercivity fractions of goethite are unlikely to be included in ***Gt***/***Hm*** paleoprecipitation estimates or the calibrations that underlie the method. Further, soils frequently contain significant concentrations of goethite and hematite in superparamagnetic grain sizes (Maher, 1998; Guyodo et al., 2006; Till et al., 2015). By definition, these grains are unable to retain remanence and would be invisible to existing ***Gt***/***Hm*** paleoprecipitation proxies. The calibration presented by Hyland et al. (2015) contains data from the literature derived mostly from XRD-based ratios, but also from magnetism-based ratios. The authors report equivalence (a nearly 1:1 relationship) between these non-magnetic and magnetic methods for 5 modern soils; however, methods based on the coercivity distributions of magnetic remanence are not sensitive

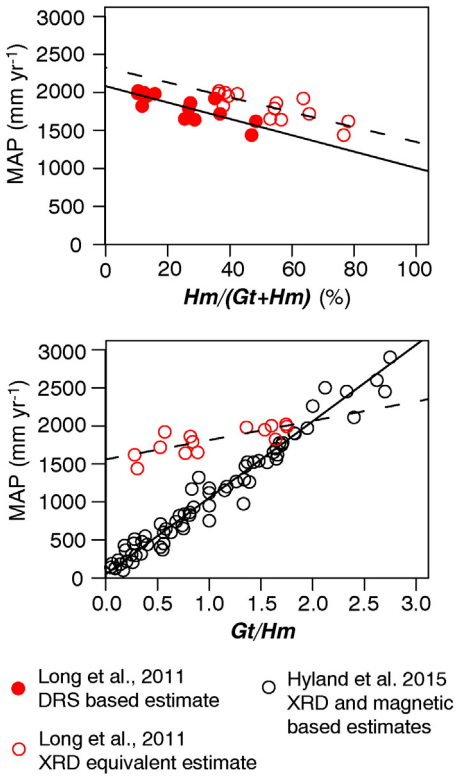

Fig. 7. Correlations between goethite and hematite abundances in modern soils with MAP. A.) Data shown in closed red symbols are from Long et al. (2011) from modern soils in South China and are derived using a DRS-based calibration between hematite and goethite weight percent and redness (see Long et al., 2011 for details). Open red symbols are corrected using the relationship described by Long et al. (2011) between DRS and XRD based estimates (see Fig. 2 in Long et al., 2011). B.) Black open circles show data from Hyland et al. (2015) for 70 modern soils with a global distribution. Methods used to derive data are a mixture of magnetic and XRD based approaches. The XRD-equivalent estimates from Long et al. (2011) have been transformed to the ***Gt/Hm*** ratio for comparison purposes. Note that only Layer II data is shown (approximated as B horizon). (For interpretation of the references to color in this figure legend, the reader is referred to the web version of this article.)

to the entire magnetic mineral assemblage in a soil, and hence, should not show equivalence with ***Gt/Hm*** estimates derived from X-ray diffraction (e.g., Hao et al., 2009).

A final concern regarding these methods is the poor correlation that the two data sets show when combined (Fig. 7). The data from Long et al. (2011) are derived from DRS based goethite and hematite abundances. Previous work has shown that DRS methods do not agree well with magnetic-based approaches to quantify antiferromagnetic abundance (Hao et al., 2009). However, even after correcting the DRS estimates to be equivalent to XRD based estimates (using a relationship provided in Long et al., 2011, see their Fig. 2), there is still a dramatic disagreement in calibrations. The calibration of Hyland et al. (2015) is far more sensitive to variation in MAP and will produce vastly different estimates of MAP than the Long et al. (2011) model for the same abundances of goethite and hematite, which should be cause for concern. Some of these discrepancies may be due to local or regional-scale processes that complicate this relationship as observed in calibrations for magnetic enhancement in loessic soils (e.g., Geiss et al., 2008 vs. Maher and Thompson, 1995) or to variations in soil moisture that are not related to precipitation (e.g., Orgeira et al., 2011). However, the scale of differences between the existing **Gt/Hm** paleoprecipitation proxies is much greater than the regional differences observed with magnetic proxies based on pedogenic enhancement of magnetite and maghemite. We highlight these variations as examples of complications that can arise when non-uniform methods are used for estimates of goethite and hematite abundances.

5.3. Recognizing error in magnetic paleoprecipitation proxies

The goal of developing suitable magnetic paleoprecipitation proxies is ultimately to use these methods to make quantitative estimates of MAP in the geologic past. It is critical that any proxy-based estimation of MAP is reported with a realistic uncertainty. Recent discussions in the literature about how best to calculate uncertainties for magnetic paleoprecipitation proxies for loessic soils show that susceptibility-based paleoprecipitation estimates have large uncertainties (e.g., Heslop and Roberts, 2013; Maher and Possolo, 2013). The uncertainties in recent ***Gt/Hm*** paleoproxies have yet to be critically evaluated (e.g., Long et al., 2011; Liu et al., 2013; Hyland et al., 2015). Considering the ambiguities associated with estimating the abundance of these minerals using magnetic methods, and the complexities in the pedogenic formation of these minerals, a responsible appraisal of the uncertainty in these methods should be a theme for future research.

6. Physical, chemical, and biological complications

6.1. Physical

Three physical factors play an important role in soil formation (Jenny, 1941) and may confound relationships between precipitation and iron oxide mineralogy: (1) duration of pedogenesis, (2) parent material, and (3) topography/soil drainage.

An important assumption for magnetic paleoprecipitation proxies is that soils reach a quasi-equilibrium state with respect to ferrimagnetic and/or antiferromagnetic mineral production (Thompson and Maher, 1995; Orgeira et al., 2011). In other words, we assume that the relative abundance of iron oxide minerals does not change after some equilibrium state has been reached within a soil, regardless of the duration of pedogenesis. For instance, alternating redox oscillations under wet/dry cycles promotes both the precipitation of new magnetite as well as the dissolution of preexisting magnetite or maghemite. If these paleoprecipitation proxies are to be useful in reconstructing environmental conditions on timescales of centuries, then the competition between precipitation and dissolution must reach steady state equilibrium on timescales of decades to centuries.

The influence of time on the magnetic properties of soils remains poorly constrained. Studies of soil chronosequences in northern California have shown that the duration of pedogenesis has a strong correlation with soil magnetism and that soils younger than ~40 ka display only minimal magnetic enhancement (Fine et al., 1989; Singer et al., 1992). This is supported by Holocene soils in the Wind River Range, Wyoming (Quinton et al., 2011) and the Chinese Loess Plateau (Vidic et al., 2004). However, others have argued that such soils have not yet attained equilibrium and that soil age is not the primary control on a soil's magnetic properties (e.g., Maher et al., 2003b). This line of reasoning is supported by observations of significant magnetic enhancement in loessic soils in the Great Plains that formed since the retreat of the last glaciation (~15 ka; Geiss et al., 2004; Geiss and Zanner, 2007). Observations of soils and paleosols within the Chinese Loess Plateau also support this interpretation (compare Vidic et al., 2004 with Maher and Hu, 2006). A study of alluvial vertisols in Texas documented magnetic enhancement that developed over the course of centuries (Fig. 7; Lindquist et al., 2011). However, recent observations of magnetism in alluvial soils developed on differently aged river terraces along the Delaware River Valley suggest that time does influence magnetic mineralogy in this system (Stinchcomb and Peppe, 2014).

These observations do not exclude the effects of time on the development of magnetic enhancement within soils, but rather suggest that the rate of magnetic enhancement in any given region is a reflection of several interconnected environmental conditions, including MAP, temperature, seasonality of precipitation, parent material, topography, and time. Thus, soils in each landscape will require their own characteristic time to equilibrate their magnetic mineral assemblages. Such regionally variable rates of magnetic enhancement are a concern for

researchers aiming to reconstruct precipitation rates from paleosols whose pedogenic equilibration rates are unknown.

The iron content of a soil's parent material is likely to be a major control on the amount of iron that is supplied to the soil solution during weathering reactions and pedogenesis. Studies using a large dataset of χ and χ_{fd} measurements in topsoil (upper 15 cm) across England and Wales have suggested that parent material is the primary control of bulk χ_{fd} in the soils of this region (Dearing et al., 1996b; Blundell et al., 2009; Boyle et al., 2010). This is consistent with soils from across Austria where parent material is important in determining the amount of ferrimagnetic mineral production via pedogenesis (Hanesch and Scholger, 2005). However, Orgeira et al. (2011) argue that the wt.% iron that is present within soils in ferrimagnetic minerals is so small (generally < 0.1 wt%) in comparison to total iron content (~2–5 wt.%) that it is unlikely that a supply of iron is a limiting factor in their formation, at least in loess derived soils (see also Maher, 1998). Instead, it is more likely that ferrimagnetic mineral formation is more closely linked to environmental factors like soil moisture (Maher, 1998; Orgeira et al., 2011). Although, total iron content may be more important for magnetic minerals that occur in greater abundance (hematite and goethite) and future work should continue to treat parent material as a potential complication in magnetic paleoprecipitation proxies.

Topography and soil drainage are two factors that might have considerable control on soil moisture, and ultimately the formation and transformation of magnetic minerals. Topography and drainage, as well as duration of pedogenesis, were factors identified as secondary controls on χ_{fd} in the dataset of English topsoil (Blundell et al., 2009; Boyle et al., 2010). Well-drained soils have higher χ_{fd}, while more poorly drained (or 'gleyed') soils have characteristically low χ_{fd} (Dearing et al., 1996b; Blundell et al., 2009; Lu et al., 2012). This is consistent with nearly all other studies to our knowledge that document magnetic enhancement. In fine-grained (clay rich) soil sequences, χ increases as you proceed downhill (de Jong et al., 1998); this pattern is reversed in soil with grain sizes dominated by coarser sands (higher χ at hilltops; de Jong et al., 2000; Blundell et al., 2009). Given these patterns, it is advisable that calibrations linking magnetic mineral assemblages to climate variables be based exclusively on soils that are well-drained and located within uniform topography. In turn, application of these proxy calibrations must be applied in the fossil record only when independent evidence exists to support similar conditions of drainage and topography at the time of soil formation.

6.2. Chemical

The chemical conditions in a soil environment influence the abiotic and biotic processes that initiate the precipitation, dissolution, and transformation of various iron oxide mineral phases. These factors include soil pH, isomorphic substitutions and ion adsorption, abundance of soil organic matter, and the concentration of molecular oxygen.

The combination of pH and oxygenation of pore spaces and fluids within a soil are two main controls on the solubility of ferrous and ferric iron. Ferric iron (Fe^{3+}) is only soluble in acidic soils (pH < ~3). In near neutral pH ranges, common in most soils, Fe^{3+} ions in solution will rapidly undergo hydrolysis to form poorly crystalline ferric iron hydroxides and ferrihydrite if the soil conditions are oxic (Colombo et al., 2013). In contrast to ferric iron, ferrous iron (Fe^{2+}) is much more soluble in soils with near neutral pH. However, if the soil solution at these pH levels is also oxygenated the Fe^{2+} ions will rapidly oxidize to Fe^{3+} and initiate mineral precipitation.

Isomorphic substitution is common in natural iron oxides. The most common ion that substitutes into Fe(III)-oxides is Al^{3+} because of its abundance in the soil environment, its similar valence state to Fe^{3+}, and its tendency towards octahedral site occupancy (Cornell and Schwertmann, 2003; Essington, 2004). Aluminum for iron substitution generally does not cause changes in structural charge, indicating that the reactivity of various iron oxides is likely to be dominated by surface area and structural vacancies (Essington, 2004). However, aluminum substitution does impact the magnetic properties of iron oxides, particularly goethite and hematite as discussed above (Murad, 1988; see Section 2). Importantly, pedogenic magnetite and maghemite are often substitution free, indicating direct in-situ formation rather than transformation from other commonly substituted iron oxides (Maher and Taylor, 1988).

Organic matter inhibits the formation of more crystalline iron oxide phases. Soils with high organic matter content tend to have more abundant iron-organic complexes and ferrihydrites. These soils require longer durations to attain equilibrium between ambient climate conditions and stable oxide phases, and are likely not as useful for magnetic paleoprecipitation proxies. For example, Histosols (wetland soils) have the highest average soil organic matter content of any soil order, and consistently display low χ (Dearing et al., 1996b; Blundell et al., 2009; Lu et al., 2012). These low χ values are likely due to a combination of reductive dissolution of preexisting stable iron oxide phases, the inhibition of ferrihydrite transformation to more stable phases by soil organic matter, and simply dilution due to the abundance of non-magnetic organic material.

6.3. Biological

Microbes play an integral role in the redox cycling of iron across a diverse range of natural settings, including soils (Colombo et al., 2013). Similar to abiotic reactions, biological processes are sensitive to soil conditions such as pH and dissolved oxygen content. Therefore, in a broad sense, physio-chemical soil conditions are the overriding control on both biotic and abiotic processes that control iron oxide mineral speciation.

As previously noted, dissimilatory iron reducing bacteria (DIRB) couple the oxidation of organic matter with the reduction of ferrous oxide minerals for metabolic energy gain (see reviews by Lovley et al., 2004; Lovley, 2013). DIRBs include those in the well-studied genera *Geobacter* and *Geothrix* among others (Lovley, 2013 provides a complete list of DIRBs). DIRB contribute to both to the dissolution of ferrous iron oxide minerals when soils become anoxic and also to the production of extracellular magnetite (see Section 5.1). However, DIRBs are typically anaerobic and occupy localized water-logged zones within a soil. As we have noted, water-logged soils that are anoxic for prolonged periods of time should be avoided in magnetic paleoprecipitation proxy calibrations.

If DIRBs are the primary drivers for the production of pedogenic magnetite in well-drained soils, which are largely oxic for long periods of time, then it follows that there must be a way for these bacteria to tolerate or avoid oxic conditions. DIRBs survive oxic conditions using a combination of at least four mechanisms. First, DIRBs preferentially occupy anoxic microenvironments, such as pore spaces within soil aggregates where anoxic conditions are more stable (Ranjard and Richaume, 2001; Hansel et al., 2008). Second, in some species of DIRBs we observe metabolic flexibility in the presence of oxygen (i.e., switching from anaerobic metabolism to aerobic; Methé et al., 2003; Lin et al., 2004; Núñez et al., 2006). Third, some DIRBs go dormant in unfavorable conditions by lowering their metabolism and energy requirements (Holmes et al., 2009; Lin et al., 2009; Mouser et al., 2009; Marozava et al., 2014). And lastly, DIRBs have been shown to secrete enzymes with a high redox potential so that their reducing potential is maintained even in microoxic conditions (Mehta-Kolte and Bond, 2012).

The rate and extent of DIRB dissolution in soils is likely to be governed by the amount of soil organic matter, humic substances within the soil (which act as electron shuttles during dissimilatory iron reduction; Nevin and Lovley, 2000; Weiss et al., 2004), and the degree of crystallinity and composition of ferrous iron oxide minerals within the soil (Bonneville et al., 2004; Roden, 2006). Predictably, high soil organic matter, high concentrations of humic acids, high reactive surface area, and low crystallinity are all associated with more rapid

rates of mineral dissolution (e.g., Emerson and Weiss, 2004; Dubinsky et al., 2010). The reduction of structural ferric iron releases Fe^{2+} ions into the soil solution (Cornell and Schwertmann, 2003) and over time scales of many hours the accumulation of Fe^{2+} in solution appears to limit the rates of DIRB dissolution (Roden, 2006).

Of importance for understanding the magnetic enhancement observed in many soils is the biotic precipitation of iron oxides, principally magnetite. Biological mineralization processes can produce magnetite intracellularly (e.g., magnetotactic bacteria) or extracellularly as has been discussed with respect to DIR bacteria (Frankel and Blakemore, 1991). The most well-known example of biologically synthesized magnetite is that of magnetotactic bacteria (see reviews by Blakemore, 1982; Moskowitz, 1995; Bazylinski et al., 2013). Magnetotactic bacteria synthesize SSD grains of magnetite (termed magnetosomes) that are encased in a protein membrane and often are aligned in chains along a common crystallographic axis (Baumgartner et al., 2013). The principle function of the magnetosomes are for navigation and orientation in a process referred to as magnetotaxis.

Magnetotactic bacteria are common in oxic-anoxic transition zones in stratified water columns or surface sediments in both freshwater and marine environments (Bazylinski et al., 2013). Fassbinder et al. (1990) discovered magnetotactic bacteria in a waterlogged soil in Germany and others have noted biogenic greigite in gley soils (Stanjek et al., 1994); however to our knowledge there has been no other report of magnetotactic bacteria in soils. Further, the amount of bacterial cells recovered by Fassbinder et al. (1990) was insufficient to have been a significant cause of magnetic enhancement (Maher, 1998). The well-developed euhedral crystals produced by magnetotactic bacteria are easily distinguishable from pedogenic magnetite using scanning electron microscopy images and by magnetic measurements (Moskowitz et al., 1993; Moskowitz, 1995). Given that inputs of magnetite into a soil by magnetotactic bacteria should be detectable by electron microscopy and by rock magnetic measurements, the rarity of magnetosomes in soils suggests that magnetotactic bacteria are not a significant source of magnetite in most soils.

7. Diagenetic concerns

There is still much to learn about the influence of post-burial diagenetic processes that occur during the transition from an active soil into a paleosol. In this review, diagenesis refers to post-burial processes excluding metamorphism.

Compaction is one of the most fundamental processes that occur to soils upon burial. Compaction in paleosols is a function of burial overburden and soil solidity (the density ratio between the soil and the solid parent material), and therefore varies between different soil orders (Sheldon and Retallack, 2001; Sheldon and Tabor, 2009). Paleosol compaction alone is not likely to influence the iron oxide mineral phases, although the extent of soil compaction will decrease the porosity and permeability, which in turn controls the exposure of magnetic minerals to potentially altering groundwater solutions.

Yet burial depths are important to the magnetic mineral assemblages in paleosols. Investigations of a sequence of Miocene to Holocene paleosols showed that increasing burial depths (range from 0 to 5 km) were associated with an increase in hematite and goethite abundance and a decrease in the SP/SSD fraction of magnetite and maghemite (Sangode et al., 2008). If the observed differences in the paleosols are due to diagenetic processes driven by overburden pressure, rather than to changing environmental conditions between the Miocene to Holocene, then these diagenetic processes may be a significant source of uncertainty when using magnetism to study paleosols from deep time. Alternatively, the observed variation in magnetic mineral assemblages with depth may reflect processes that are simply related to burial time. Disentangling a paleosol's primary recording of the environmental conditions in which it equilibrated from the distorting effects of diagenesis remains a difficult challenge to the paleoclimate community.

Gleying (prolonged reduction under water-logged conditions) of previously well-drained soils upon burial can occur in paleosols that subside below the water table, and can create anoxic conditions in paleosol pore spaces (Retallack, 1991). Post-burial gleying often causes dissolution of ferric iron oxides and may decrease the preservation of magnetic minerals in paleosols. Typically, post-burial gleying results in fine iron oxide coatings on ped surfaces, in particular coatings that span microfractures through pedogenic structures (Nordt et al., 2011). Iron oxides precipitated in root casts, usually surrounding a gray interior core, are common evidence of surface gleying (PiPujol and Buurman, 1997; Kraus and Hasiotis, 2006). If significant post-burial gleying has occurred, then it is likely that this will disturb the original assemblage of pedogenic magnetic minerals. For practical purposes, large root trace zones or other prominent redoximorphic features should be avoided when sampling paleosols for magnetic analyses.

The dehydration of goethite and recrystallization to hematite has been proposed as one mechanism for the post-burial reddening of many terrestrial red beds and paleosols (Retallack, 1991). Post-burial dehydration reactions should impact iron oxide minerals pervasively within a paleosol, given the timescales over which these processes occur (Kraus and Hasiotis, 2006). The presence of goethite and hematite mixtures in paleosols, as well as their complex color assemblages, has been used as evidence of the minimal role played by diagenetic transformations of iron oxides in paleosols from the Bighorn Basin, Wyoming (Kraus and Hasiotis, 2006). However, recent recovery of sediment cores by the Bighorn Basin Coring Project shows that oxidative weathering fronts penetrate nearly 30 m below the Earth's surface (Clyde et al., 2013). This recent observation suggests that oxidative surficial weathering significantly alters the magnetic mineral assemblage of paleosols exposed as outcrops. However, the extent of this process has yet to be quantified in detail.

Several studies have documented that diagenetic processes can create secondary chemical remagnetizations in terrestrial sandstone and carbonate deposits within orogenic belts (e.g., McCabe and Elmore, 1989; Banerjee et al., 1997; Katz et al., 2000; Cox et al., 2005; Tohver et al., 2008). Possible mechanisms for chemical remagnetization include the dissolution and remobilization of Fe^{2+} by thermal maturation of organic matter (Banerjee et al., 1997), and the release of Fe^{2+} during the illitization of Fe-rich smectite clay minerals (McCabe and Elmore, 1989; Woods et al., 2002; Cox et al., 2005). Both of these processes are associated with the authigenic production of magnetite. Paleomagnetic studies of the Chinese Loess Plateau have explored remagnetization in loessic deposits (e.g., Løvlie et al., 2011). However, to our knowledge these mechanisms have not been considered in the context of paleosol diagenesis, particularly with respect to magnetic minerals produced during pedogenesis. These processes are likely only relevant for paleosols that have subsided to burial depths of at least 2–3 km (the depth associated with illitization of smectites; Woods et al., 2002; Cox et al., 2005).

Diagenesis may also be microbially mediated. Microbes, particularly Archaea, can exist in some of the most extreme environments on Earth. This holds true for the subsurface, including buried paleosols (e.g., Khomutova et al., 2014). Dormant microbial communities have been recovered in buried paleosols of age 1–4 Ma (Brockman et al., 1992) and portions of these communities can be re-animated with the onset of favorable conditions (Demkina et al., 2008). A more extreme example of subsurface microbial life is the recovery of very fine grained magnetite associated with gas and oil deposits ~ 6.7 km below the Earth's surface that are attributed to Fe(III)-reducing bacteria (Gold, 1992). Thermophillic Fe(III)-reducing bacteria have been recovered from ~2.1 km below the surface in the Cretaceous sediments of the Piceance Basin of western Colorado (Liu, 1997). The presence of Fe (III)-reducing bacteria in subsurface deposits may aid in the degradation of organic matter and the addition of Fe^{2+} into groundwater. This microbial activity has the potential to alter the primary magnetic mineralogy of paleosols because magnetite is an associated byproduct of Fe

(III)-reduction via DIRB. While it is probable that microbes contribute to the post-burial destruction or addition of ferrimagnetic minerals in some systems, the magnitude of this contribution remains unknown.

Post-burial gleying of originally well-drained soils has been invoked to explain low χ (~5–20 $\times 10^{-8}$ m^3 kg^{-1}) in Precambrian and early Paleozoic paleosols, as compared to temperate modern soils whose χ values tend to be higher (~500 $\times 10^{-8}$ m^3 kg^{-1}) (Maher, 1998; Retallack et al., 2003). Similarly low χ values (2–20 $\times 10^{-8}$ m^3 kg^{-1}) have been documented in the Pennsylvanian Roca Shale (Rankey and Farr, 1997) as well as loessite–paleosol sequences in the Permian Maroon Formation (Soreghan et al., 1997; Cogoini et al., 2001; Soreghan et al., 2002; Tramp et al., 2004) and the upper-Paleozoic lower Cutler beds of Utah (Cogoini et al., 2001). Despite the low values of χ in many of these paleosols, many of these studies have concluded that the magnetic minerals preserved within these soils are pedogenic (e.g., Rankey and Farr, 1997; Cogoini et al., 2001; Tramp et al., 2004). Further, the observed enhancement ratio of susceptibility in paleosols to loessite for the loessite–paleosol sequences in the Maroon Formation (Cogoini et al., 2001; Tramp et al., 2004) are comparable to the χ enhancement in modern loessic soils of the U.S. Great Plains (Geiss et al., 2008). Comparable measures of magnetic enhancement between modern soils and paleosols alone should not be taken to indicate that similar climatic regimes were present during soil formation. However, observable magnetic enhancement in ancient paleosols does provide a positive outlook for rock magnetic studies by suggesting that primary magnetic enhancement signals are preserved to some extent in even the oldest paleosols.

8. Challenges for future work

Despite the interrelated complications associated with the physical, chemical, and biological evolution of soils and paleosols there is considerable promise that quantitative magnetic methods can be developed to better interpret records of magnetic mineral assemblages preserved in paleosols. Future work should target two key themes:

1. The community needs to quantify more precisely the relationships between the formation of iron oxide minerals in modern soils and ambient environmental parameters such as precipitation, temperature, and seasonality across a range of environments. We encourage studies that explore more broadly how these environmental parameters act to control soil moisture, which is the ultimate driver for magnetic mineral production, as well as other parameters such as duration of pedogenesis. Much of the existing work has focused on loess-derived soils, which while informative, represent only a small fraction of possible soil orders. Future work ought to expand and build upon existing methods to determine how applicable magnetic paleoprecipitation proxies might be in different soil orders and from more variable geographical locations.
2. The rock magnetic community needs to develop clear and easily followed experimental protocols for determining the mass or volume abundances of individual iron oxide minerals within soils. Such methods will be essential for properly calibrating paleoproxy tools based on hematite and goethite abundance, as well as for determining the fraction of pedogenic magnetite/maghemite that has been preserved within a paleosol. In order for methods to be widely applicable it will be necessary that future researchers be able to directly replicate the methods of previous studies to ensure that parameters used in proxies are uniformly measured and calculated.

Acknowledgments

The authors wish to thank Brandy Toner and Jake Bailey for discussion that helped to shape early versions of this work. Subir Banerjee, Christoph Geiss, and David Heslop contributed thoughtful comments that greatly improved this review. DPM acknowledges funding provided by the Richard C. Dennis Fellowship through the UMN Department of Earth Sciences and the UMN Stanwood Johnston Fellowship. This is IRM contribution 1510.

Appendix A. Primer on mineral and environmental magnetism

A.1. Magnetic susceptibility

Soils represent a complex mixture of various organic compounds and mineral constituents of various grain size and composition (including both iron oxides and all other soil minerals). When soil is placed in an applied magnetic field ($\boldsymbol{H}$) it will produce an induced magnetization ($\boldsymbol{M}$). The volume magnetic susceptibility (κ) of that soil is expressed as the induced magnetization divided by $\boldsymbol{H}$:

$$\kappa = \boldsymbol{M}/\boldsymbol{H} \tag{A1}$$

where $\boldsymbol{M}$ and $\boldsymbol{H}$ both have units of A m^{-1} and κ is dimensionless (Evans and Heller, 2003; Tauxe et al., 2014). Mass normalized susceptibility (χ), which is predominantly used in soil and paleosol studies, is defined as the volume magnetic susceptibility divided by the density (ρ) of the material (Thompson and Oldfield, 1986):

$$\chi = \kappa/\rho \tag{A2}$$

where χ has units of m^3 kg^{-1}. Reported values of χ are frequently measures of the low-field (<800 A m^{-1}) magnetic susceptibility (χ_{lf}). We note that susceptibility is defined using the applied magnetic field, $\boldsymbol{H}$ (A m^{-1}) while the induced magnetic field ($\boldsymbol{B}$, units of Tesla) can be derived using the relationship $\boldsymbol{B} = \mu_o \boldsymbol{H}$, where μ_o is the permeability of free space ($4\pi \cdot 10^{-7}$ H m^{-1}; Stacey and Banerjee, 1974). Most recent studies report magnetic properties with respect to $\boldsymbol{B}$ fields, and we will use $\boldsymbol{B}$ predominately through the remainder of this appendix and throughout the main body of the review.

Measured values of χ represent contributions of induced magnetizations from diamagnetic, paramagnetic, and various ferromagnetic minerals in a soil. The distinction between these mineral types is related to crystal structure and the interactions between unpaired electron spins in neighboring atoms (Harrison and Feinberg, 2009; Tauxe et al., 2014). Diamagnetic minerals (e.g., quartz, carbonates) have very weak, negative induced magnetizations ($\chi \sim -8 \times 10^{-8}$ m^3 kg^{-1}). Paramagnetic minerals (e.g., ferromagnesian silicate minerals) produce a weak, positive magnetization that varies linearly with applied magnetic field strength. Both diamagnetic and paramagnetic minerals have no net magnetization in the absence of an applied field.

Ferromagnetic materials (e.g., pure iron) produce a permanent spontaneous magnetization in the absence of an applied field that arises due to a parallel coupling of magnetic moments produced by unpaired electron spins within a mineral's crystal lattice. Perfect antiferromagnetic minerals should have an antiparallel arrangement of magnetic sub-lattices and no net magnetization in the absence of an applied field. However, due to defects in crystal structures and spin canting, so-called antiferromagnetic minerals (e.g., hematite and goethite) produce permanent magnetizations as well as weak positive induced magnetization (χ ~ 60–70 $\times 10^{-8}$ m^3 kg^{-1}; Maher, 2007). Ferrimagnetic minerals (e.g., magnetite and maghemite) have unequal antiparallel arrangements of electron spin moments and characteristically produce both strong permanent and induced magnetizations (e.g., χ of magnetite is ~500 $\times 10^{-6}$ m^3 kg^{-1}; Maher, 2007).

Due to the order of magnitude difference in strength of the induced magnetizations between ferrimagnetic minerals and all other soil constituents (e.g., antiferromagnetic, paramagnetic, and diamagnetic minerals), χ is often viewed as a rough proxy for the abundance of ferrimagnetic minerals, when present, regardless of grain size and composition. However, in some clay rich soils paramagnetic susceptibility

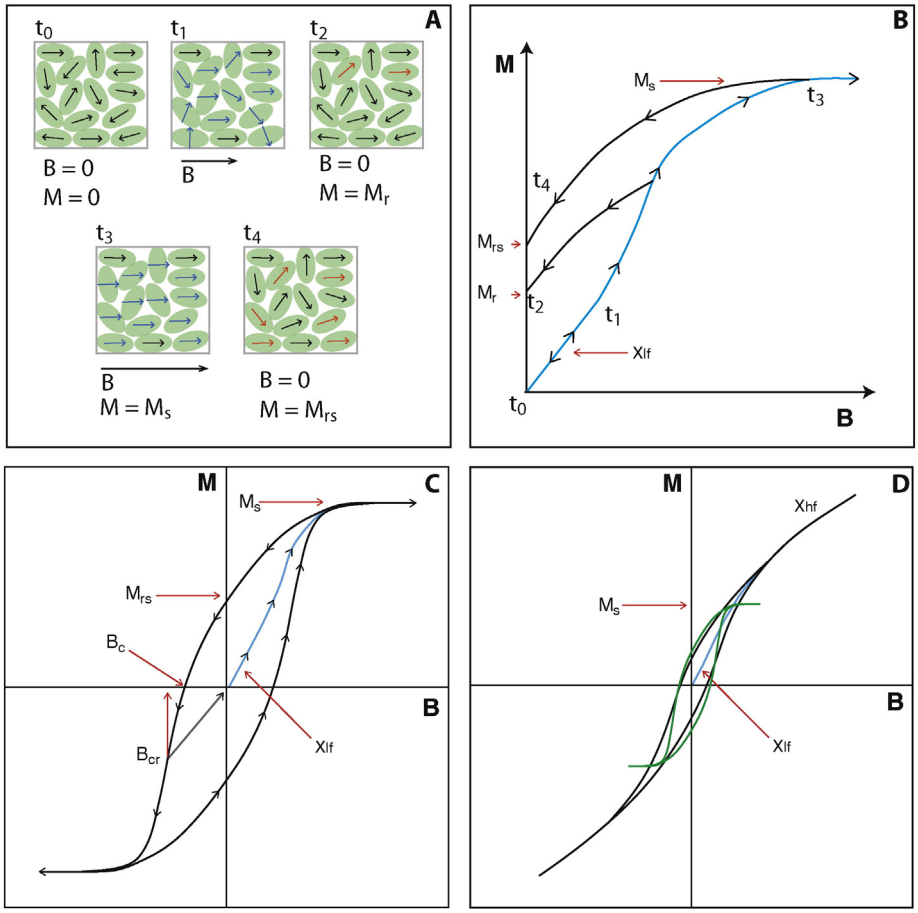

Fig. A.1. Magnetic hysteresis and coercivity. A. Schematic representation of the magnetic moments (arrows) of an ensemble of individual single domain grains (represented as green ovals). Paired with the magnetization curve in B it is possible to follow the effects of increasing the applied field to the magnetization. From t_0 to t_1 some of the individual magnetic moments begin to align with the magnetic field (indicated by blue arrows within grains at t_1), which results in a measurable low-field susceptibility (χ). If the applied field remains less than the coercivities of all individual grains, the magnetic moments for all particles will return to their original state at t_0 when the field is removed. In the case that the applied field exceeds the coercivities of some individual grains, those magnetic moments will permanently change to be more in line with the field direction (orange arrows at t_2) and there will be a remanent magnetization ($\boldsymbol{M_r}$) when the applied field is removed. Further increases in the magnetic field will continue to align the magnetic moment of individual grains until a maximum alignment is reached. The magnetization measured in the presence of this saturating field is the saturation magnetization ($\boldsymbol{M_s}$). The magnetization measured in the absence of the field, after saturation, is the remanent saturation magnetization ($\boldsymbol{M_{rs}}$) and is shown at t_4. C. The application of an increasing field in the opposite direction will eventually reduce the induced magnetization to zero, and the strength of this field is referred to as the bulk coercivity ($\boldsymbol{B_c}$). A slightly larger field is required to reduce the remanent magnetization to zero ($\boldsymbol{B_{cr}}$). $\boldsymbol{B_{cr}}$ is a measure of the direct field that must be applied to remagnetize individual particles in the ensemble such that the remanent magnetization is zero. The outline of the black curve is referred to as a major hysteresis loop. D. The hysteresis loop shown in C is an idealized loop where all measured particles are capable of retaining a remanence. The slope of the line above the loop closure in D is referred to as high field susceptibility ($\boldsymbol{\chi_{hf}}$) and represents the net induced contribution from paramagnetic and diamagnetic materials in a specimen (both of which respond linearly in applied magnetic fields). Typically this contribution is mathematically removed during data processing and a ferromagnetic hysteresis loop is obtained that is similar to that shown in C (green loop in D). Figures and captions adapted from Tauxe et al. (2014).

can be dominant (Dearing et al., 1996a; Yamazaki and Ioka, 1997; Jordanova and Jordanova, 1999).

A.2. Magnetic grain size

The magnetic properties of iron oxide minerals in soils are highly dependent on the grain sizes of individual mineral particles. The smallest iron oxide nanoparticles (<30 nm; all grain size boundaries discussed here are specific to magnetite; Dunlop, 1973; Butler and Banerjee, 1975) are superparamagnetic (SP). SP particles are uniformly magnetized, however they are unable to hold a permanent magnetization because thermal energy randomizes any magnetic alignment at room temperature in the absence of an applied field. As grain size increases (30–~75 nm; Dunlop, 1973; Butler and Banerjee, 1975) magnetic particles have a stable, uniform magnetization and are referred to as stable single domain (SSD). These grains are capable of accurately recording the direction and strength of the Earth's magnetic field, and their presence is critical to paleomagnetic studies. For larger mineral particles (>300 nm–100 μm; Worm and Markert, 1987; Heider et al., 1992), it becomes more energetically favorable for grains to form multiple zones of uniform magnetization separated by highly mobile domain walls, and mineral particles of this size are referred to as multidomain (MD). Notably, grains that fall in the grain size range between SSD and MD have variable magnetic behavior and are referred to as pseudo-single domain (PSD). As will be highlighted below (and throughout the main portions of this review), the interpretation of a soil's magnetism is informed in large part by the distribution of magnetic domain states (SP, SSD, PSD, and MD) that are present.

A.3. Magnetic remanence and hysteresis

If a soil specimen is exposed to a weak magnetic field, then the measured magnetization relative to the field is expressed as the low field χ (discussed above). If the applied field is then reduced to zero, then the material's induced magnetization returns to zero (e.g., magnetization goes from t_1 back to t_0 in Fig. A.1A and B). If the applied field is large enough to "flip" the magnetic moments of some individual ferrimagnetic or antiferromagnetic SSD grains and/or unpin magnetic domain walls in MD mineral grains, then the specimen will retain a permanent magnetization parallel to the applied field when the field is removed.

This permanent magnetization is referred to as magnetic remanence (M_r, see Fig. A.1; recall that SP grains do not retain remanence). M_r acquired in response to a direct field at room temperature is referred to as an isothermal remanent magnetization ($IRM_{x\ mT}$, where the subscript describes the strength of the applied field used to impart remanence in units of milliTesla). A specimen typically reaches saturation magnetization, where the magnetizations of its constituent grains are maximally aligned with the applied field (Fig. A.1A, B) in large applied fields (generally greater than or equal to the 1 T available in most laboratories). These fields are strong enough to saturate 'soft' ferrimagnetic minerals, such as magnetite and maghemite, but larger fields are required to saturate 'hard' magnetic minerals like hematite and goethite (e.g., Maher et al., 2004; Rochette et al., 2005). When a sufficiently strong field is used to completely saturate a specimen's magnetization, the specimen will retain a saturation remanence when the field is removed (saturation isothermal remanent magnetization, ***SIRM*** or saturation remanent magnetization M_{rs}; see Fig. A.1). Application of a field in the opposite direction will begin to reduce the magnetization of the sample from ***SIRM*** towards saturation in the opposite direction.

The strength of the field required to reduce a saturated specimen's induced magnetization to zero is referred to as the bulk coercivity (B_c; Fig. A.1C). If a specimen's remanence is monitored as successively larger, negative fields are momentarily applied, then we can determine the coercivity of remanence (B_{cr}; Fig. A.1C), which corresponds to the field that reduces the specimen's M_r from ***SIRM*** to zero. By definition, B_{cr} is equal to or greater than B_c. At the scale of an individual, uniaxial SSD grain, coercivity is defined as the field required to irreversibly 'flip' the direction of magnetization. For a natural specimen, B_c can be thought of as the field required to reverse the magnetic moments of enough grains within a specimen such that half of the magnetization is aligned in the opposite direction of the saturating field. Coercivity for individual grains of ferrimagnetic and antiferromagnetic minerals varies greatly, and is influenced by mineralogy, shape, volume, and internal strain. The distribution of coercivity values present within an individual specimen is critical to several magnetic methods (e.g., coercivity unmixing and first order reversal curves) used to differentiate between various sub-populations of magnetic iron oxides (discussed in Section 4).

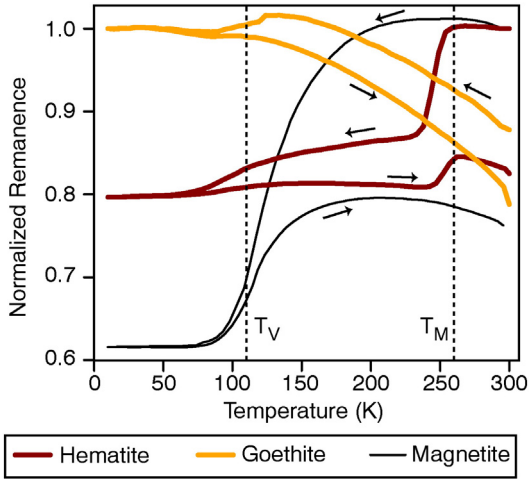

Fig. A.3. Room temperature (RT) ***SIRM*** for synthetic specimen of magnetite, goethite (with trace magnetite), and hematite. Note the characteristic loss of remanence at the Verwey transition for magnetite (T_V; indicated with dashed line at 110 K) and the Morin transition for hematite (T_M; indicated with dashed line at 260 K). Goethite is characterized by an increase in remanence upon cooling. Note that the Verwey transition is apparent from this synthetic powder sample, indicating a trace amount of magnetite contamination in this specimen. All data displayed here is freely available from the Institute for Rock Magnetism online Rock Magnetic Bestiary (http://www.irm.umn.edu/bestiary2/). Remanence values for hematite and magnetite are normalized to initial ***SIRM*** values measured at 300 K. Goethite values are normalized to the ***IRM*** value measured at 10 K.

A separate form of magnetic remanence, anhysteretic remanent magnetization (***ARM***), is used extensively in environmental magnetic studies of soils (e.g., Geiss and Zanner, 2007; Geiss et al., 2008). In most rock magnetic laboratories, an ***ARM*** is imparted to a specimen using a magnetizer that is capable of simultaneously generating a small direct field (~8–16 × 10^4 A m^{-1}; referred to as H_{bias}, similar in magnitude to the Earth's magnetic field) as well as a much stronger alternating field (AF), whose peak strength, frequency, and attenuation rate are controlled by the user. As the alternating field oscillates back and forth, it forces the magnetization of magnetic grains within the specimen to align in both the positive and negative directions of the attenuating wave form according to their own individual coercivities. The small direct field acts to bias the alignment of the grains' magnetizations as the alternating field decays. If no direct field bias is used, and the peak alternating field strength is greater than the coercivity of all grains in the specimen, then half of the magnetization will be positive with the other half being negative, ultimately resulting in a net zero remanence (i.e., AF demagnetization; Tauxe et al., 2014). ***ARM*** is commonly normalized by H_{bias}, in which case it is referred to as the ***ARM*** susceptibility (χ_{ARM}), with units of m^3 kg^{-1}. ***ARM***, χ_{ARM}, and the ratio of ***ARM*** (or χ_{ARM}) to ***IRM*** are excellent indicators of the presence of SSD grains in a sample (e.g., Maher, 1988) due to the fact that MD grains generally have exceedingly low coercivities and are unable to retain any significant ***ARM***.

As a soil specimen is exposed to increasing fields its constituent magnetic minerals will eventually become saturated, where the magnetization of each grain has reached maximum alignment with the applied field. At field strengths higher than saturation, a specimen's magnetization will continue to increase linearly as magnetic moments in paramagnetic and purely antiferromagnetic minerals become progressively more aligned with the applied field. The slope of the linear increase is referred to as the high field susceptibility (χ_{hf}; see Fig. 1D) and the difference between χ and χ_{hf} yields the contribution of ferrimagnetic minerals (regardless of grain size) to the susceptibility and is termed 'ferrimagnetic susceptibility' (χ_{ferri}; Evans and Heller, 2003).

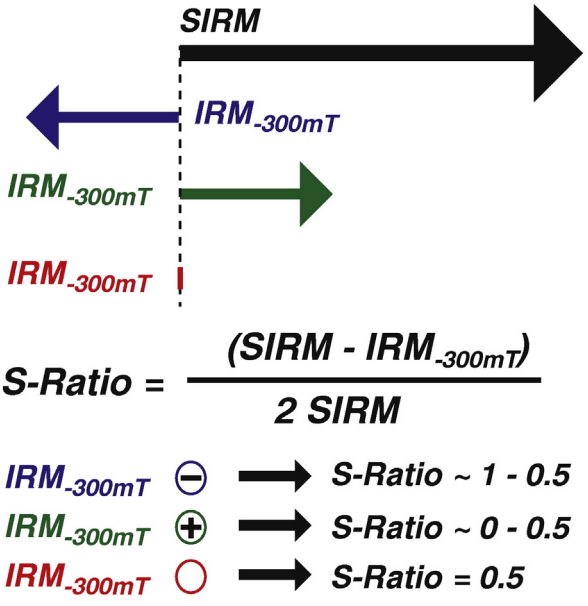

Fig. A.2. Schematic representation of the magnetizations and formula used to calculate the ***S-Ratio***. If the ***S-Ratio*** is calculated according to the equation shown here (Eq. (A3) in text) then values between 1 and 0.5 indicate greater than 50% of the remanence is held by soft ferrimagnetic minerals. An ***S-Ratio*** of 0.5 is a special case such that exactly 50% of remanence is held by ferrimagnets and 50% is held by antiferromagnets. An ***S-Ratio*** of less than 0.5 indicates that antiferromagnets hold more than 50% of the remanence measurable in a specimen. See text for more details.

A.4. S-Ratio and L-Ratio

The ***S-Ratio*** is a common parameter that is used in environmental magnetism to quantify the proportion of hard and soft magnetic minerals in natural sediments (e.g., Stober and Thompson, 1979; Bloemendal et al., 1992). The ***S-Ratio*** originally was expressed as the ratio of an ***IRM*** acquired at some non-saturating backfield (often −300 mT or −100 mT) measured after the acquisition of an ***SIRM*** (e.g., $-\boldsymbol{IRM}_{-300\ mT}/\boldsymbol{SIRM}$; Stober and Thompson, 1979). Values close to unity are interpreted to indicate that remanence within a specimen is held primarily by soft magnetic minerals.

In most cases in which natural sediment or soil specimens are studied, there will be a measurable remanence in the backfield direction after the application of a small backfield (the blue arrow in Fig. A.2) because of the strong remanence held by even trace amounts of soft ferrimagnets. In the traditional treatment of the ***S-Ratio***, $\boldsymbol{IRM}_{-300\ mT}$ will represent the contribution of soft minerals to the initially measured ***SIRM***. However, in theory the true contribution of the soft minerals to ***SIRM*** is one half the original ***SIRM*** minus $\boldsymbol{IRM}_{-300\ mT}$. This is highlighted by the special case that $\boldsymbol{IRM}_{-300\ mT}$ is zero (shown as red in Fig. A.2). If the original ***SIRM*** is held equally by a soft and hard component, the application of a backfield will reduce the specimen's remanence to zero and a traditional ***S-Ratio*** will be zero. For these reasons, the ***S-Ratio*** is often calculated following the definition of Bloemendal et al. (1992):

$$\boldsymbol{S-Ratio} = 0.5 * (\boldsymbol{SIRM} - \boldsymbol{IRM}_{-300\ mT})/\boldsymbol{SIRM} \quad \text{(A3)}$$

where the numerator now represents the true contribution from the soft mineral component to ***SIRM*** (the compliment to ***HIRM***). If calculated according to Eq. (A3), values for the ***S-Ratio*** between 1 and 0.5 would indicate greater than 50% remanence held by a soft component, values less than 0.5 would indicate greater than 50% remanence held by a hard component (green arrow in Fig. A.2), and a value of 0.5 would indicate remanence held equally by soft and hard minerals. We stress that magnetic based comparisons of relative contributions to remanence are not equivalent to mass or volume estimates of these minerals (see Section 4.4). For example, a 0.5 ***S-Ratio*** (according to Eq. (A3)) would indicate an order of magnitude difference between the mass/volume fractions of the hard antiferromagnets with respect to magnetite/maghemite in order for the bulk remanence held by these components to be equivalent (Bloemendal et al., 1992).

Liu et al. (2007a) proposed the ***L-Ratio*** as a complimentary measure to aide in the interpretation of both the ***S-Ratio*** and ***HIRM***. The ***L-Ratio*** is defined as the ratio of the resultant $\boldsymbol{IRM}_{1\ T}$ magnetization remaining after AF demagnetization at two intermediate fields (e.g., 300 and 100 mT):

$$\boldsymbol{L-Ratio} = \boldsymbol{IRM}_{AF@300\ mT}/\boldsymbol{IRM}_{AF@100\ mT} \quad \text{(A4)}$$

where values close to 1 indicate higher $\boldsymbol{B}_{cr}$ values. For a given set of samples, if the ***L-Ratio*** remains relatively constant it can be taken that coercivity distributions are constant and that traditional interpretations of ***HIRM*** and the ***S-Ratio*** are valid. In the case that the ***L-Ratio*** is variable for a set of samples, it is suggested to indicate that coercivity distributions are variable within individual specimens and that variations in the ***HIRM*** and the ***S-Ratio*** are likely due to coercivity variations rather than relative differences in the contributions of these minerals to overall remanence.

A.5. Some useful high and low temperature measurements

Lowrie (1990) proposed orthogonal ***IRM*** acquisition followed by thermal demagnetization as a way to isolate a soft (~120 mT), intermediate (~400 mT), and hard (5 T) component within a specimen. Monitoring the remanence loss as temperature increases allows for identification of major slope changes indicating remanence lost at characteristic transition temperatures for ferromagnetic minerals (e.g. Curie temperature, T_C for ferrimagnets and Néel Temperature, T_N for antiferromagnets; see Lowrie, 1990; Tauxe et al., 2014 for more details related to T_C and T_N). In the case that thermal demagnetization confirms that individual mineral components hold remanence only along one orthogonal axis (e.g., soft axis is held entirely by magnetite, intermediate only by hematite, and hard only by goethite), an absolute value for the remanence held by individual mineral components can be attained. However, because variability in coercivity can cause overlap between coercivity distributions of mineral phases (e.g., low coercivity hematite and hard maghemite) and the potential to induce mineral transformations at elevated temperature, care needs to be taken in order to assign a specific mineral phase to the remanence held along each axis.

Low temperature remanence cycling is a useful alternative to high temperature cycling because it avoids thermal alteration of mineral phases. Using a Magnetic Properties Measurement System (MPMS; Quantum Designs Inc., San Diego CA) it is possible to impart large direct current fields (~5–7 T) and to observe induced magnetization and remanence while temperature is cycled from room temperature (RT, ~300 K) down to ~10 K. A typical routine used to characterize magnetic mineralogy is a RT-***SIRM*** (shown in Fig. A.3; see Lascu and Feinberg, 2011). An initial ***IRM*** at some saturating field (~2.5–7 T) is applied while the specimen is at room temperature. Following this treatment, remanence is monitored while the temperature is decreased to ~10 K and subsequently increased back to 300 K. Hematite displays a large drop in remanence at the Morin transition (T_M, ~260 K; see Fig. A.3) while magnetite loses remanence at the Verwey transition (T_V, ~110 K; see Fig. 5). Goethite is characterized by a factor of ~2 increase in remanence on cooling (Lascu and Feinberg, 2011). We note that in many soils the Morin transition is suppressed due to defects and substitutions common to soil hematite; however it is possible to identify hematite by inspection of the first derivative of the RT-***SIRM*** curve where sharp deviations of the derivative curve at T_M are indicative of hematite (see Lascu and Feinberg, 2011; Morón et al., 2013).

For magnetic mineral characterization, particularly for the identification of goethite and hematite within a specimen, RT-***SIRM*** is a particularly useful tool that ought to be applied in the study of soils. It is possible to quantify the remanence held by each mineral phase by conducting a series of RT-***SIRM*** experiments that are separated by sequential demagnetization experiments aimed to "remove" the magnetization of individual mineral phases. Demagnetization of the soft ferrimagnets can be achieved by AF demagnetization (either via traditional methods in a U-channel magnetometer or via the "oscillation" mode of a MPMS), while goethite can be demagnetized by heating of the sample to 400 K (above the T_N of goethite, but not sufficiently high to induce mineral transformations; see Guyodo et al., 2006 for a detailed example).

References

Abrajevitch, A., van der Voo, R., Rea, D.K., 2009. Variations in relative abundances of goethite and hematite in Bengal Fan sediments: climatic vs. diagenetic signals. Mar. Geol. 267, 191–206. http://dx.doi.org/10.1016/j.margeo.2009.10.010.

Alekseev, A.O., Alekseeva, T.V., Maher, B.A., 2003. Magnetic properties and mineralogy of iron compounds in steppe soils. Eurasian Soil Sci. 36, 59–70.

Balsam, W.L., Ellwood, B.B., Ji, J., Williams, E.R., Long, X., El Hassani, A., 2011. Magnetic susceptibility as a proxy for rainfall: worldwide data from tropical and temperate climate. Quat. Sci. Rev. 30, 2732–2744. http://dx.doi.org/10.1016/j.quascirev.2011.06.002.

Balsam, W., Ji, J., Chen, J., 2004. Climatic interpretation of the Luochuan and Lingtai loess sections, China, based on changing iron oxide mineralogy and magnetic susceptibility. Earth Planet. Sci. Lett. 223, 335–348. http://dx.doi.org/10.1016/j.epsl.2004.04.023.

Banerjee, S., Elmore, R.D., Engel, M.H., 1997. Chemical remagnetization and burial diagenesis: testing the hypothesis in the Pennsylvanian Belden Formation, Colorado. J. Geophys. Res. 102, 24825–24842. http://dx.doi.org/10.1029/97JB01893.

Banerjee, S.K., Moskowitz, B.M., 1985. Ferrimagnetic properties of magnetite. In: Kirschvink, J.L., Jones, D.S., MacFadden, B.J. (Eds.), Magnetite Biomineralization and Magnetoreception in Organisms Spring U.S., pp. 17-41.

Barron, V., Torrent, J., 2002. Evidence for a simple pathway to maghemite in Earth and Mars soils. Geochim. Cosmochim. Acta 66, 2801–2806.

Barron, V., Torrent, J., de Grave, E., 2003. Hydromaghemite, an intermediate in the hydrothermal transformation of 2-line ferrihydrite into hematite. Am. Mineral. 88, 1679–1688.

Baumgartner, J., Morin, G., Menguy, N., Gonzalez, T.P., Widdrat, M., Cosmidis, J., Faivre, D., 2013. Magnetotactic bacteria form magnetite from a phosphate-rich ferric hydroxide via nanometric ferric (oxyhydr)oxide intermediates. Proc. Natl. Acad. Sci. 110, 14883–14888. http://dx.doi.org/10.1073/pnas.1307119110.

Bazylinski, D.A., Lefevre, C.T., Schuler, D., 2013. Magnetotactic Bacteria. In: Rosenberg, E., DeLong, E.F., Lory, S., Stackebrandt, E., Thompson, F. (Eds.), The Prokaryotes: Prokaryotic Physiology and Biochemistry. Springer, Berlin, Berlin, pp. 453–494.

Begét, J.E., Stone, D.B., Hawkins, D.B., 1990. Paleoclimatic forcing of magnetic susceptibility variations in Alaskan loess during the late Quaternary. Geology 18, 40–43. http://dx.doi.org/10.1130/0091-7613(1990)018<0040.

Blakemore, R.P., 1982. Magnetotactic bacteria. Annu. Rev. Microbiol. 36, 217–238.

Bloemendal, J., King, J.W., Hall, F.R., Doh, S.J., 1992. Rock magnetism of Late Neogene and Pleistocene deep-sea sediments: relationship to sediment source, diagenetic processes, and sediment lithology. J. Geophys. Res. 97, 4361–4375. http://dx.doi.org/10.1029/91JB03068.

Blundell, A., Dearing, J.A., Boyle, J.F., Hannam, J.A., 2009. Controlling factors for the spatial variability of soil magnetic susceptibility across England and Wales. Earth Sci. Rev. 95, 158–188. http://dx.doi.org/10.1016/j.earscirev.2009.05.001.

Bonneville, S., Vancappellen, P., Behrends, T., 2004. Microbial reduction of iron(III) oxyhydroxides: effects of mineral solubility and availability. Chem. Geol. 212, 255–268. http://dx.doi.org/10.1016/j.chemgeo.2004.08.015.

Boyle, J.F., Dearing, J.A., Blundell, A., Hannam, J.A., 2010. Testing competing hypotheses for soil magnetic susceptibility using a new chemical kinetic model. Geology 38, 1059–1062. http://dx.doi.org/10.1130/G31514.1.

Brockman, F.J., Kieft, T.L., Fredrickson, J.K., Bjornstad, B.N., Li, S.W., Spangenburg, W., Long, P.E., 1992. Microbiology of vadose zone paleosols in south-central Washington State Hanford Site. Microb. Ecol. 23, 279–301.

Butler, R.F., Banerjee, S.K., 1975. Theoretical single-domain grains size range in magnetite and titanomagnetite. J. Geophys. Res. 80, 4049–4058. http://dx.doi.org/10.1029/JB080i029p04049.

Cabello, E., Morales, M.P., Serna, C.J., Barron, V., Torrent, J., 2009. Magnetic enhancement during the crystallization of ferrihydrite at 25 and 50 °C. Clay Clay Miner. 57, 46–53. http://dx.doi.org/10.1346/CCMN.2009.0570105.

Carter-Stiglitz, B., Banerjee, S.K., Gourlan, A., Oches, E., 2006. A multi-proxy study of Argentina loess: marine oxygen isotope stage 4 and 5 environmental record from pedogenic hematite. Palaeogeogr. Palaeoclimatol. Palaeoecol. 239, 45–62. http://dx.doi.org/10.1016/j.palaeo.2006.01.008.

Chen, T., Xu, H., Xie, Q., Chen, J., Ji, J., Lu, H., 2005. Characteristics and genesis of maghemite in Chinese loess and paleosols: mechanism for magnetic susceptibility enhancement in paleosols. Earth Planet. Sci. Lett. 240, 790–802. http://dx.doi.org/10.1016/j.epsl.2005.09.026.

Childs, C.W., 1992. Ferrihydrite: a review of structure, properties and occurrence in relation to soils. Z. Pflanzenernähr. Bodenkd. 155, 441–448.

Cismasu, A.C., Levard, C., Michel, F.M., Brown, G.E., 2013. Properties of impurity-bearing ferrihydrite II: insights into the surface structure and composition of pure, Al- and Si-bearing ferrihydrite from Zn(II) sorption experiments and Zn K-edge X-ray absorption spectroscopy. Geochim. Cosmochim. Acta 119, 46–60. http://dx.doi.org/10.1016/j.gca.2013.05.040.

Cismasu, A.C., Michel, F.M., Stebbins, J.F., Levard, C., Brown, G.E., 2012. Properties of impurity-bearing ferrihydrite I: effects of Al content and precipitation rate on the structure of 2-line ferrihydrite. Geochim. Cosmochim. Acta 92, 275–291. http://dx.doi.org/10.1016/j.gca.2012.06.010.

Cismasu, A.C., Michel, F.M., Tcaciuc, A.P., Tyliszczak, T., Brown Jr., G.E., 2011. Composition and structural aspects of naturally occurring ferrihydrite. Compt. Rendus Geosci. 343, 210–218. http://dx.doi.org/10.1016/j.crte.2010.11.001.

Clyde, W.C., Gingerich, P.D., Wing, S.L., Röhl, U., Westerhold, T., Bowen, G., Johnson, K., Baczynski, A.A., Diefendorf, A., McInerney, F., Schnurrenberger, D., Noren, A., Brady, K., 2013. Bighorn Basin Coring Project (BBCP): a continental perspective on early Paleogene hyperthermals. Sci. Drill. 16, 21–31. http://dx.doi.org/10.5194/sd-16-21-2013.

Cogoini, M., Elmore, R.D., Soreghan, G.S., Lewchuk, M.T., 2001. Contrasting rock-magnetic characteristics of two Upper Paleozoic loessite–paleosol profiles. Phys. Chem. Earth Solid Earth Geod. 26, 905–910.

Collinson, D.W., 1968. An estimate of the haematite content of sediments by magnetic analysis. Earth Planet. Sci. Lett. 4, 417–421. http://dx.doi.org/10.1016/0012-821X(68)90015-0.

Colombo, C., Palumbo, G., He, J.-Z., Pinton, R., Cesco, S., 2013. Review on iron availability in soil: interaction of Fe minerals, plants, and microbes. J. Soils Sediments 14, 538–548. http://dx.doi.org/10.1007/s11368-013-0814-z.

Cornell, R.M., Schwertmann, U., 2003. The Iron Oxides: Structures, Properties, Reactions, Occurences, and Uses. Wiley-VCH.

Cox, E., Elmore, R.D., Evans, M., 2005. Paleomagnetism of Devonian red beds in the Appalachian Plateau and valley and ridge provinces. J. Geophys. Res. 110, B08102. http://dx.doi.org/10.1029/2005JB003640.

Das, S., Hendry, M.J., Essilfie-Dughan, J., 2011. Transformation of two-line ferrihydrite to goethite and hematite as a function of pH and temperature. Environ. Sci. Technol. 45, 268–275. http://dx.doi.org/10.1021/es101903y.

Day, R., Fuller, M., Schmidt, V.A., 1977. Hysteresis properties of titanomagnetites: grain-size and compositional dependence. Phys. Earth Planet. In. 13, 260–267. http://dx.doi.org/10.1016/0031-9201(77)90108-X.

Dearing, J.A., Dann, R.J.L., Hay, K., Lees, J.A., Loveland, P.J., Maher, B.A., Grady, K.O., Survey, S., Mk, B., 1996a. Frequency-dependent susceptibility measurements of environmental materials. Geophys. J. Int. 124, 228–240.

Dearing, J.A., Hay, K.L., Baban, S.M.J., Huddleston, A.S., Wellington, E.M.H., Loveland, P.J., 1996b. Magnetic susceptibility of soil: an evaluation of conflicting theories using a national data set. Geophys. J. Int. 127, 728–734. http://dx.doi.org/10.1111/j.1365-246X.1996.tb04051.x.

Dekkers, M.J., 1989. Magnetic properties of natural goethite—I: grain-size dependence of some low- and high-field related rock magnetic parameters measured at room temperature. Geophys. J. Int. 97, 323–340. http://dx.doi.org/10.1111/j.1365-246X.1989.tb00504.x.

Demkina, T.S., Khomutova, T.E., Kashirskaya, N.N., Demkina, E.V., Stretovich, I.V., El-Registan, G.I., Demkin, V.A., 2008. Age and activation of microbial communities in soils under burial mounds and in recent surface soils of steppe zone. Eurasian Soil Science 41, 1439–1447. http://dx.doi.org/10.1134/S1064229308130139.

Dubinsky, E.A., Silver, W.L., Firestone, M.K., 2010. Tropical forest soil microbial communities couple iron and carbon biogeochemistry. Ecology 9, 2604–2612.

Dunlop, D.J., 1973. Superparamagnetic and single-domain threshold sizes in magnetite. J. Geophys. Res. 78, 459–471.

Dunlop, D.J., 2002. Theory and application of the Day plot (M_{rs}/M_s versus H_{cr}/H_c) 2: application to data for rocks, sediments, and soils. J. Geophys. Res. 107, 1–15.

Dunlop, D.J., Özdemir, O., 2001. Rock Magnetism: Fundamentals and Frontiers. v. 3. Cambridge University Press.

Dunlop, D.J., Özdemir, O., 2006. Magnetic memory and coupling between spin-canted and defect magnetism in hematite. J. Geophys. Res. 111 (B12S03). http://dx.doi.org/10.1029/2006JB004555.

Egli, R., 2003. Analysis of the field dependence of remanent magnetization curves. J. Geophys. Res. 108, 1–25. http://dx.doi.org/10.1029/2002JB002023.

Egli, R., 2004a. Characterization of individual rock magnetic components by analysis of remanence curves, 1. Unmixing natural sediments. Stud. Geophys. Geod. 48, 391–446. http://dx.doi.org/10.1023/B:SGEG.0000020839.45304.6d.

Egli, R., 2004b. Characterization of individual rock magnetic components by analysis of remanence curves. 2. Fundamental properties of coercivity distributions. Phys. Chem. Earth 29, 851–867. http://dx.doi.org/10.1016/j.pce.2004.04.001.

Emerson, D., Weiss, J.V., 2004. Bacterial iron oxidation in circumneutral freshwater habitats: findings from the field and the laboratory. Geomicrobiol J. 21, 405–414.

Eronen, J., Puolamäki, K., Liu, L., 2010a. Precipitation and large herbivorous mammals I: estimates from present-day communities. Evol. Ecol. Res. 12, 217–233.

Eronen, J.T., Puolamäki, K., Liu, L., Lintulaakso, K., Damuth, J., Janis, C., Fortelius, M., 2010b. Precipitation and large herbivorous mammals II: application to fossil data. Evol. Ecol. Res. 12, 235–248.

Essington, M.E., 2004. Soil and Water Chemistry: An Integrative Approach. CRC Press, Boca Raton, FL.

Eusterhues, K., Wagner, F.E., Häusler, W., Hanzlik, M., Knicker, H., Totsche, K.U., Kögel-Knabner, I., Schwertmann, U., 2008. Characterization of ferrihydrite-soil organic matter coprecipitates by X-ray diffraction and Mössbauer spectroscopy. Environ. Sci. Technol. 42, 7891–7897.

Evans, M.E., and Heller, F., 2003. Environmental Magnetism: Principles and Applications of Enviromagnetics. Elsevier Science (USA), San Diego, CA.

Fassbinder, J.W.E., Stanjek, H., Vali, H., 1990. Occurrence of magnetic bacteria in soil. Nature 343, 161–162.

Fassbinder, J.W.E., Stanjek, H., 1994. Magnetic properties of biogenic soil greigite (Fe_3S_4). Geophys. Res. Lett. 21, 2349–2352. http://dx.doi.org/10.1029/94GL02506.

Fine, P., Singer, M.J., Ven, R.L.A., Verosub, K., Southard, R.J., 1989. Role of pedogenesis in distribution of magnetic susceptibility in two California chronosequences. Geoderma 44, 287–306.

Fitzpatrick, R.W., 1988. Iron compounds as indicators of pedogenic processes: examples from the Southern Hemisphere. In: Stucki, J.W., Goodman, B.A., Schwertmann, U. (Eds.), Iron in Soils and Clay Minerals. D. Rediel Publishing Company, The Netherlands, pp. 351–396.

France, D.E., Oldfield, F., 2000. Identifying goethite and hematite from rock magnetic measurements of soils and sediments. J. Geophys. Res. 105, 2781–2795.

Frankel, R.B., Blakemore, R.P., 1991. Iron Biominerals. Plenum Press, New York.

Ge, K., Williams, W., Liu, Q., Yu, Y., 2014. Effects of the core-shell structure on the magentic properties of partially oxidized magentite grains: experimental and micromagnetic investigations. Geochem. Geophys. Geosyst. 15, 2021–2038. http://dx.doi.org/10.1002/2014GC005265.

Geiss, C.E., Egli, R., Zanner, C.W., 2008. Direct estimates of pedogenic magnetite as a tool to reconstruct past climates from buried soils. J. Geophys. Res. 113, B11102. http://dx.doi.org/10.1029/2008JB005669.

Geiss, C.E., Zanner, C.W., 2006. How abundant is pedogenic magnetite? Abundance and grain size estimates for loessic soils based on rock magnetic analyses. J. Geophys. Res. 111 (B12S21). http://dx.doi.org/10.1029/2006JB004564.

Geiss, C.E., Zanner, C.W., 2007. Sediment magnetic signature of climate in modern loessic soils from the Great Plains. Quat. Int. 162-163, 97–110. http://dx.doi.org/10.1016/j.quaint.2006.10.035.

Geiss, C.E., Zanner, C.W., Banerjee, S.K., Joanna, M., 2004. Signature of magnetic enhancement in a loessic soil in Nebraska, United States of America. Earth Planet. Sci. Lett. 228, 355–367. http://dx.doi.org/10.1016/j.epsl.2004.10.011.

Gold, T., 1992. The deep, hot biosphere. Proc. Natl. Acad. Sci. U. S. A. 89, 6045–6049.

Guyodo, Y., LaPara, T.M., Anschutz, A.J., Penn, R.L., Banerjee, S.K., Geiss, C.E., Zanner, W., 2006. Rock magnetic, chemical and bacterial community analysis of a modern soil from Nebraska. Earth Planet. Sci. Lett. 251, 168–178. http://dx.doi.org/10.1016/j.epsl.2006.09.005.

Guyodo, Y., Sainctavit, P., Arrio, M., Carvallo, C., Penn, R.L., Erbs, J.J., Forsberg, B.S., Morin, G., Maillot, F., Lagroix, F., Bonville, P., Wilhelm, F., and Rogalev, A., 2012. X-ray magnetic circular dichroïsm provides strong evidence for tetrahedral iron in ferrihydrite. Geochem. Geophys. Geosyst.. 13, 9 p., doi: http://dx.doi.org/10.1029/2012GC004182.

Hanesch, M., Scholger, R., 2005. The influence of soil type on the magnetic susceptibility measured throughout soil profiles. Geophys. J. Int. 161, 50–56. http://dx.doi.org/10.1111/j.1365-246X.2005.02577.x.

Hansel, C.M., Fendorf, S., Jardine, P.M., Francis, C.A., 2008. Changes in bacterial and archaeal community structure and functional diversity along a geochemically variable soil profile. Appl. Environ. Microbiol. 74, 1620–1633. http://dx.doi.org/10.1128/AEM.01787-07.

Hao, Q., Oldfield, F., Bloemendal, J., Torrent, J., Guo, Z., 2009. The record of changing hematite and goethite accumulation over the past 22 Myr on the Chinese Loess Plateau from magnetic measurements and diffuse reflectance spectroscopy. J. Geophys. Res. Solid Earth 114, 1–18. http://dx.doi.org/10.1029/2009JB006604.

Harrison, R.J., Feinberg, J.M., 2009. Mineral magnetism: Providing new insights into geoscience processes. Elements 5, 209–215. http://dx.doi.org/10.2113/gselements.5.4.209.

Heider, F., Dunlop, D.J., Soffel, H.C., 1992. Low-temperature and alternating field demagnetization of saturation remanence and thermoremanence in magnetite grains (0.037 μm to 5 mm). J. Geophys. Res. 97, 9371–9381.

Heller, F., Liu, T., 1986. Palaeoclimate and sedimentary history from magnetic susceptibility of loess in China. Geophys. Res. Lett. 13, 1169–1172.

Heslop, D., Dekkers, M.J., Kruiver, P.P., Van Oorschot, I.H.M., 2002. Analysis of isothermal remanent magnetization acquisition curves using the expectation–maximization algorithm. Geophys. J. Int. 148, 58–64. http://dx.doi.org/10.1046/j.0956-540x.2001.01558.x.

Heslop, D., McIntosh, G., Dekkers, M.J., 2004. Using time- and temperature-dependent Preisach models to investigate the limitations of modeling isothermal remanent magnetization acquisition curves with cumulative log Gaussian functions. Geophys. J. Int. 157, 55–63. http://dx.doi.org/10.1111/j.1365-246X.2004.02155.x.

Heslop, D., Dillon, M., 2007. Unmixing magnetic remanence curves without a priori knowledge. Geophys. J. Int. 170, 556–566. http://dx.doi.org/10.1111/j.1365-246X.2007.03432.x.

Heslop, D., Roberts, A.P., 2013. Calculating uncertainties on predictions of palaeoprecipitation from the magnetic properties of soils. Global Planet. Change 110, 379–385. http://dx.doi.org/10.1016/j.gloplacha.2012.11.013.

Heslop, D., 2015. Numerical strategies for magnetic mineral unmixing. Earth Sci. Rev. 150, 256–284. http://dx.doi.org/10.1016/j.earscirev.2015.07.007.

Holmes, D.E., O'Neil, R.A., Chavan, M.A., N'Guessan, L.A., Vrionis, H.A., Perpetua, L.A., Larrahondo, M.J., DiDonato, R., Liu, A., Lovley, D.R., 2009. Transcriptome of *Geobacter uraniireducens* growing in uranium-contaminated subsurface sediments. ISME J. 3, 216–230. http://dx.doi.org/10.1038/ismej.2008.89.

Hu, P., Liu, Q., Heslop, D., Roberts, A.P., Jin, C., 2015. Soil moisture balance and magnetic enhancement in loess–paleosol sequences from the Tibetan Plateau and Chinese Loess Plateau. Earth Planet. Sci. Lett. 409, 120–132. http://dx.doi.org/10.1016/j.epsl.2014.10.035.

Hunt, C.P., Moskowitz, B.M., Banerjee, S.K., 1995. Magnetic properties of rocks and minerals. In: Ahrens, T.J. (Ed.), Rock Physics and Phase Relations: A Handbook of Physical Constants AGU Reference Shelf, ISN 1080-305X, pp. 189-204.

Hyland, E., Sheldon, N.D., Van der Voo, R., Badgley, C., Abrajevitch, A., 2015. A new paleoprecipitation proxy based on soil magnetic properties: implications for expanding paleoclimate reconstructions. Geol. Soc. Am. Bull. http://dx.doi.org/10.1130/B31207.1.

Jackson, M., Moskowitz, B., Rosenbaum, J., Kissel, C., 1998. Field-dependence of AC susceptibility in titanomagnetites. Earth Planet. Sci. Lett. 157, 129–139. http://dx.doi.org/10.1016/S0012-821X(98)00032-6.

Jambor, J.L., Dutrizac, J.E., 1998. Occurrence and constitution of natural and synthetic ferrihydrite, a widespread iron oxyhydroxide. Chem. Rev. 98, 2549–2586.

Janney, D.E., Cowley, J.M., Buseck, P.R., 2000. Structure of synthetic 2-line ferrihydrite by electron nanodiffraction. Am. Mineral. 85, 1180–1187.

Jenny, H., 1941. Factors of Soil Formation. McGraw-Hill, New York.

Jiamao, H., Houyuan, L., Naiquin, W., Zhengtang, G., 1996. The magnetic susceptibility of modern soils in China and its use for paleoclimate reconstruction. Stud. Geophys. Geod. 40, 262–275. http://dx.doi.org/10.1007/BF02300742.

de Jong, E., Nestor, P., Pennock, D., 1998. The use of magnetic susceptibility to measure long-term soil redistribution. Catena 32, 23–35. http://dx.doi.org/10.1016/S0341-8162(97)00051-9.

de Jong, E., Pennock, D., Nestor, P., 2000. Magnetic susceptibility of soils in different slope positions in Saskatchewan, Canada. Catena 40, 291–305. http://dx.doi.org/10.1016/S0341-8162(00)00080-1.

Jordanova, D., Jordanova, N., 1999. Magnetic characteristics of different soil types from Bulgaria. Stud. Geophys. Geod. 43, 303–318. http://dx.doi.org/10.1023/A:1023398728538.

Kampf, N., Schwertmann, U., 1983. Goethite and hematite in a climosequence in southern Brazil and their application in classification of kaolinitic soils. Geoderma 29, 27–39.

Katz, B., Douglas, R., Cogoini, M., Engel, M.H., Ferry, S., 2000. Associations between burial diagenesis of smectite, chemical remagnetization, and magnetite authigenesis in the Vocontian trough, SE France. J. Geophys. Res. 105, 851–868. http://dx.doi.org/10.1029/1999JB900309.

Khomutova, T.E., Demkina, T.S., Demkin, V.A., 2014. The state of microbial communities in buried paleosols in relation to prevailing climates in steppes of the Lower Volga region. Quat. Int. 324, 115–123. http://dx.doi.org/10.1016/j.quaint.2014.01.039.

Kraus, M.J., Hasiotis, S.T., 2006. Significance of different modes of rhizolith preservation to interpreting paleoenvironmental and paleohydrologic settings: examples from Paleogene paleosols, Bighorn Basin, Wyoming, U.S.A. J. Sediment. Res. 76, 633–646. http://dx.doi.org/10.2110/jsr.2006.052.

Kruiver, P.P., Dekkers, M.J., Heslop, D., 2001. Quantification of magnetic coercivity components by the analysis of acquisition curves of isothermal remanent magnetization. Earth Planet. Sci. Lett. 189, 269–276.

Kukla, G., Heller, F., Ming, L.X., Chun, X.T., Sheng, L.T., Sheng, A.Z., 1988. Pleistocene climates in China dated by magnetic susceptibility. Geology 16, 811–814. http://dx.doi.org/10.1130/0091-7613(1988)016<0811:PCICDB>2.3.CO;2.

Lagroix, F., Banerjee, S.K., 2002. Paleowind directions from magnetic fabric of loess profiles in central Alaska. Earth Planet. Sci. Lett. 195, 99–112. http://dx.doi.org/10.1016/S0012-821X(01)00564-7.

Lagroix, F., Banerjee, S.K., 2004. The regional and temporal significance of primary aeolian magnetic fabrics preserved in Alaskan loess. Earth Planet. Sci. Lett. 225, 379–395. http://dx.doi.org/10.1016/j.epsl.2004.07.003.

Lascu, I., Feinberg, J.M., 2011. Speleothem magnetism. Quat. Sci. Rev. 30, 330623–330624 p. ence ReviewssM., 20117.003.f prima.

LeBorgne, E., 1955. Susceptibilité magnétiques anormale du sol superficiel. Ann. Geophys. 11, 399–419.

LeBorgne, E., 1960. Influence du feu sur les proprience magnétiques du sol et sur celles du schist et du granite. Ann. Geophys. 16, 159–195.

Lin, W.C., Coppi, M.V., Lovley, D.R., 2004. *Geobacter sulfurreducens* can grow with oxygen as a terminal electron acceptor. Appl. Environ. Microbiol. 70, 2525–2528. http://dx.doi.org/10.1128/AEM.70.4.2525.

Lin, B., Westerhoff, H.V., Röling, W.F.M., 2009. How Geobacteraceae may dominate subsurface biodegradation: physiology of *Geobacter metallireducens* in slow-growth habitat-simulating retentostats. Environ. Microbiol. 11, 2425–2433. http://dx.doi.org/10.1111/j.1462-2920.2009.01971.x.

Lindquist, A.K., Feinberg, J.M., Waters, M.R., 2011. Rock magnetic properties of a soil developed on an alluvial deposit at Buttermilk Creek, Texas, USA. Geochem. Geophys. Geosyst. 12 (Q12Z36) 10.1029/2011GC003848.

Liu, S.V., 1997. Thermophilic Fe(III)-reducing bacteria from the deep subsurface: the evolutionary implications. Science 277, 1106–1109. http://dx.doi.org/10.1126/science.277.5329.1106.

Liu, Q., Banerjee, S.K., Jackson, M.J., 2002. A new method in mineral magnetism for the separation of weak antiferromagnetic signal from a strong ferrimagnetic background. Geophys. Res. Lett. 29, 1–4. http://dx.doi.org/10.1029/2002GL014699.

Liu, Q., Barrón, V., Torrent, J., Eeckhout, S.G., Deng, C., 2008. Magnetism of intermediate hydromaghemite in the transformation of 2-line ferrihydrite into hematite and its paleoenvironmental implications. J. Geophys. Res. 113 (B01103). http://dx.doi.org/10.1029/2007JB005207.

Liu, Q., Deng, C., Torrent, J., Zhu, R., 2007a. Review of recent developments in mineral magnetism of the Chinese loess. Quat. Sci. Rev. 26, 368–385. http://dx.doi.org/10.1016/j.quascirev.2006.08.004.

Liu, Q., Hu, P., Torrent, J., Barrón, V., Zhao, X., Jiang, Z., Su, Y., 2010. Environmental magnetic study of a Xeralf chronosequence in northwestern Spain. Indications for pedogenesis. Palaeogeogr. Palaeoclimatol. Palaeoecol. 293, 144–156. http://dx.doi.org/10.1016/j.palaeo.2010.05.008.

Liu, Z., Liu, Q., Torrent, J., Barrón, V., Hu, P., 2013. Testing the magnetic proxy χ_{fd}/HIRM for quantifying paleoprecipitation in modern soil profiles from Shaanxi Province, China. Glob. Planet. Chang. 110, 368–378. http://dx.doi.org/10.1016/j.gloplacha.2013.04.013.

Liu, Q., Roberts, A.P., Larrasoaña, J.C., Banerjee, S.K., Guyodo, Y., Tauxe, L., Oldfield, F., 2012. Environmental magnetism: principles and applications. Rev. Geophys. 50, RG4002. http://dx.doi.org/10.1029/2012RG000393.1.

Liu, Q., Roberts, A.P., Torrent, J., Horng, C.S., and Larrasoaña, J.C., 2007b. What do the HIRM and S-ratio really measure in environmental magnetism? Geochem. Geophys. Geosyst.. 8, Q09011, http://dx.doi.org/10.1029/2007GC001717.

Liu, X., Rolph, T., Bloemednal, J., Shaw, J., Liu, T., 1995. Quantitative estimates of palaeoprecipitation at Xifeng, in the Loess Plateau of China. Palaeogeogr. Palaeoclimatol. Palaeoecol. 113, 243–248. http://dx.doi.org/10.1016/0031-0182(95)00053-O.

Liu, Q., Torrent, J., Yu, Y., Deng, C., 2004. Mechanism of the parasitic remanence of aluminous goethite [α-(Fe, Al)OOH]. J. Geophys. Res. B: Solid Earth 109, 1–8. http://dx.doi.org/10.1029/2004JB003352.

Liu, Q., Yu, Y., Torrent, J., Roberts, A.P., Pan, Y., Zhu, R., 2006. Characteristic low-temperature magnetic properties of aluminous goethite [α-(Fe, Al)OOH] explained. J. Geophys. Res. B: Solid Earth 111, 1–12. http://dx.doi.org/10.1029/2006JB004560.

Long, X., Ji, J., Balsam, W., 2011. Rainfall-dependent transformations of iron oxides in a tropical saprolite transect of Hainan Island, South China: spectral and magnetic measurements. J. Geophys. Res. 116, F03015. http://dx.doi.org/10.1029/2010JF001712.

Lovley, D., 2013. Dissimilatory Fe(III)- and Mn(IV)-reducing prokaryotes. In: Rosenberg, E., DeLong, E.F., Lory, S., Stackebrandt, E., Thompson, F. (Eds.), The Prokaryotes — Prokaryotic Physiology and Biochemistry. Springer, Berlin, Berlin, pp. 287–308.

Lovley, D.R., Holmes, D.E., Nevin, K.P., 2004. Dissimilatory Fe(III) and Mn(IV) reduction. Adv. Microb. Physiol. 49, 219–286. http://dx.doi.org/10.1016/S0065-2911(04)49005-5.

Lovley, D.R., Stolz, J.F., Nord, G.L., Phillips, E.J.P., 1987. Anaerobic production of magnetite by a dissimilatory iron-reducing microorganism. Nature 330, 252–254.

Løvlie, R., Wang, R., Wang, X., 2011. In situ remagnetization experiments of loess on the Chinese Loess Plateau: evidence for localized post-depositional remanent magnetization. Geochem. Geophys. Geosyst. 12, 1–18. http://dx.doi.org/10.1029/2011GC003830.

Lowrie, W., 1990. Identification of ferromagnetic minerals in a rock by coercivity and unblocking temperature properties. Geophys. Res. Lett. 17, 159–162.

Lu, S.G., Zhu, L., Yu, J.Y., 2012. Mineral magnetic properties of Chinese paddy soils and its pedogenic implications. Catena 93, 9–17. http://dx.doi.org/10.1016/j.catena.2012.01.002.

Lyons, R., Tooth, S., Duller, G.A.T., 2014. Late Quaternary climatic changes revealed by luminescence dating, mineral magnetism and diffuse reflectance spectroscopy of river terrace palaeosols: a new form of geoproxy data for the southern African interior. Quat. Sci. Rev. 95, 43–59. http://dx.doi.org/10.1016/j.quascirev.2014.04.021.

Ma, M., Liu, X., Pillans, B.J., Hu, S., Lu, B., Liu, H., 2013. Magnetic properties of Dashing Rocks loess at Timaru, South Island, New Zealand. Geophys. J. Int. 195, 75–85. http://dx.doi.org/10.1093/gji/ggt206.
Maher, B.A., 1988. Magnetic properties of some synthetic sub-micron magnetites. Geophys. J. Int. 94, 83–96. http://dx.doi.org/10.1111/j.1365-246X.1988.tb03429.x.
Maher, B.A., 1998. Magnetic properties of modern soils and Quaternary loessic paleosols: paleoclimatic implications. Palaeogeogr. Palaeoclimatol. Palaeoecol. 137, 25–54. http://dx.doi.org/10.1016/S0031-0182(97)00103-X.
Maher, B.A., 2007. Environmental magnetism and climate change. Contemp. Phys. 48, 247–274. http://dx.doi.org/10.1080/00107510801889726.
Maher, B.A., 2011. The magnetic properties of Quaternary aeolian dusts and sediments, and their palaeoclimatic significance. Aeolian Res. 3, 87–144. http://dx.doi.org/10.1016/j.aeolia.2011.01.005.
Maher, B.A., Alekseev, A., Alekseeva, T., 2003a. Magnetic mineralogy of soils across the Russian Steppe: climatic dependence of pedogenic magnetite formation. Palaeogeogr. Palaeoclimatol. Palaeoecol. 201, 321–341. http://dx.doi.org/10.1016/S0031-0182(03)00618-7.
Maher, B.A., Alekseev, A., Alekseeva, T., 2002. Variation of soil magnetism across the Russian steppe: its significance for use of soil magnetism as a palaeorainfall proxy. Quat. Sci. Rev. 21, 1571–1576. http://dx.doi.org/10.1016/S0277-3791(02)00022-7.
Maher, B.A., Hu, M., 2006. A high-resolution record of Holocene rainfall variations from the western Chinese Loess Plateau: antiphase behaviour of the African/Indian and East Asian summer monsoons. The Holocene 16, 309–319. http://dx.doi.org/10.1191/0959683606hl929rp.
Maher, B.A., Karloukovski, V.V., Mutch, T.J., 2004. High-field remanence properties of synthetic and natural submicrometre haematites and goethites: significance for environmental contexts. Earth Planet. Sci. Lett. 226, 491–505. http://dx.doi.org/10.1016/j.epsl.2004.05.042.
Maher, B.A., MengYu, H., Roberts, H.M., Wintle, A.G., 2003b. Holocene loess accumulation and soil development at the western edge of the Chinese Loess Plateau: implications for magnetic proxies of palaeorainfall. Quat. Sci. Rev. 22, 445–451. http://dx.doi.org/10.1016/S0277-3791(02)00188-9.
Maher, B.A., Possolo, A., 2013. Statistical models for use of palaeosol magnetic properties as proxies of palaeorainfall. Global Planet. Change 111, 280–287. http://dx.doi.org/10.1016/j.gloplacha.2013.09.017.
Maher, B.A., Taylor, R.M., 1988. Formation of ultrafine-grained magnetite in soils. Nature 336, 368–370.
Maher, B.A., Thompson, R., 1991. Mineral magnetic record of the Chinese loess and paleosols. Geology 19, 3–6. http://dx.doi.org/10.1130/0091-7613(1991)019<0003.
Maher, B.A., Thompson, R., 1992. Paleoclimatic significance of the mineral magnetic record of the Chinese loess and paleosols. Quatern. Res. 37, 155–170.
Maher, B.A., Thompson, R., 1995. Paleorainfall reconstructions from pedogenic magnetic susceptibility variations in the Chinese loess and paleosols. Quat. Int. 44, 383–391.
Maher, B.A., Thompson, R., Zhou, L.P., 1994. Spatial and temporal reconstructions of changes in the Asian palaeomonsoon: a new mineral magnetic approach. Earth Planet. Sci. Lett. 125, 461–471. http://dx.doi.org/10.1016/0012-821X(94)90232-1.
Maillot, F., Morin, G., Wang, Y., Bonnin, D., Ildefonse, P., Chaneac, C., Calas, G., 2011. New insight into the structure of nanocrystalline ferrihydrite: EXAFS evidence for tetrahedrally coordinated iron(III). Geochim. Cosmochim. Acta 75, 2708–2720. http://dx.doi.org/10.1016/j.gca.2011.03.011.
Manceau, A., 2012. Comment on "direct observation of tetrahedrally coordinated Fe(III) in ferrihydrite". Environ. Sci. Technol. 46, 6882–6884. http://dx.doi.org/10.1021/es303084e.
Marozava, S., Röling, W.F.M., Seifert, J., Küffner, R., von Bergen, M., Meckenstock, R.U., 2014. Physiology of *Geobacter metallireducens* under excess and limitation of electron donors. Part II. Mimicking environmental conditions during cultivation in retentostats. Syst. Appl. Microbiol. 37, 287–295. http://dx.doi.org/10.1016/j.syapm.2014.02.005.
Martin-Hernandez, F., García-Hernández, M.M., 2010. Magnetic properties and anisotropy constant of goethite single crystals at saturating high fields. Geophys. J. Int. 181, 756–761. http://dx.doi.org/10.1111/j.1365-246X.2010.04566.x.
Martin-Hernandez, F., Guerrero-Suárez, S., 2012. Magnetic anisotropy of hematite natural crystals: high field experiments. Int. J. Earth Sci. 101, 637–647. http://dx.doi.org/10.1007/s00531-011-0665-z.
McCabe, C., Elmore, R.D., 1989. The occurrence and origin of Late Paleozoic remagnetization in the sedimentary rocks of North America. Rev. Geophys. 27, 471–494.
Mehta-Kolte, M.G., Bond, D.R., 2012. *Geothrix fermentans* secretes two different redox-active compounds to utilize electron acceptors across a wide range of redox potentials. Appl. Environ. Microbiol. 78, 6987–6995. http://dx.doi.org/10.1128/AEM.01460-12.
Methé, B.A., Nelson, K.E., Eisen, J.A., Paulsen, I.T., Nelson, W., Heidelberg, J.F., Wu, D., Wu, M., Ward, N., Beanan, M.J., Dodson, R.J., Madupu, R., Brinkac, L.M., Daugherty, S.C., et al., 2003. Genome of *Geobacter sulfurreducens*: metal reduction in subsurface environments. Science 302, 1967–1969. http://dx.doi.org/10.1126/science.1088727.
Michel, F.M., Barrón, V., Torrent, J., Morales, M.P., Serna, C.J., Boily, J.-F., Liu, Q., Ambrosini, A., Cismasu, A.C., Brown, G.E., 2010. Ordered ferrimagnetic form of ferrihydrite reveals links among structure, composition, and magnetism. Proc. Natl. Acad. Sci. U. S. A. 107, 2787–2792. http://dx.doi.org/10.1073/pnas.0910170107.
Michel, F.M., Ehm, L., Antao, S.M., Lee, P.L., Chupas, P.J., Liu, G., Strongin, D.R., Schoonen, M.A.A., Phillips, B.L., Parise, J.B., 2007. The structure of ferrihydrite, a nanocrystalline material. Science 316, 1726–1729. http://dx.doi.org/10.1126/science.1142525.
Morón, S., Fox, D.L., Feinberg, J.M., Jaramillo, C., Bayona, G., Montes, C., Bloch, J.I., 2013. Climate change during the Early Paleogene in the Bogotá Basin (Colombia) inferred from paleosol carbon isotope stratigraphy, major oxides, and environmental magnetism. Palaeogeogr. Palaeoclimatol. Palaeoecol. 388, 115–127. http://dx.doi.org/10.1016/j.palaeo.2013.08.010.
Moskowitz, B.M., 1995. Biomineralization of magnetic minerals. Rev. Geophys. 33, 123–128. http://dx.doi.org/10.1029/95RG00443.
Moskowitz, B.M., Frankel, R.B., Bazylinski, D.A., 1993. Rock magnetic criteria for the detection of biogenic magnetite. Earth Planet. Sci. Lett. 120, 283–300.
Mouser, P.J., Holmes, D.E., Perpetua, L.A., DiDonato, R., Postier, B., Liu, A., Lovley, D.R., 2009. Quantifying expression of *Geobacter* spp. oxidative stress genes in pure culture and during in situ uranium bioremediation. ISME J. 3, 454–465. http://dx.doi.org/10.1038/ismej.2008.126.
Mullins, C.E., 1977. Magnetic susceptibility of soil and its significance in soil science — a review. J. Soil Sci. 28, 223–246. http://dx.doi.org/10.1111/j.1365-2389.1977.tb02232.x.
Murad, E., 1988. Properties and behavior of iron oxides as determined by Mossbauer spectroscopy. In: Stucki, J.W., Goodman, B.A., Schwertmann, U. (Eds.), Iron in Soils and Clay Minerals. D. Rediel Publishing Company, The Netherlands, pp. 309–350.
Nevin, K.P., Lovley, D.R., 2000. Potential for nonenzymatic reduction of Fe(III) via electron shuttling in subsurface sediments. Environ. Sci. Technol. 34, 2472–2478. http://dx.doi.org/10.1021/es991181b.
Nordt, L.C., Dworkin, S.I., Atchley, S.C., 2011. Ecosystem response to soil biogeochemical behavior during the Late Cretaceous and early Paleocene within the western interior of North America. Geol. Soc. Am. Bull. 123, 1745–1762. http://dx.doi.org/10.1130/B30365.1.
Núñez, C., Esteve-núñez, A., Giometti, C., Tollaksen, S., Khare, T., Lin, W., Lovley, D.R., Methé, B.A., 2006. DNA microarray and proteomic analyses of the RpoS regulon in *Geobacter sulfurreducens*. J. Bacteriol. 188, 2792–2800. http://dx.doi.org/10.1128/JB.188.8.2792.
Oches, E.A., Banerjee, S.K., 1996. Rock-magnetic proxies of climate change from loess-paleosol sediments of the Czech Republic. Studia Geophysica Geodedica 40, 287–300. http://dx.doi.org/10.1007/BF02300744.
Orgeira, M.J., Egli, R., Compagnucci, R.H., 2011. A quantitative model of magnetic enhancement in loessic soils. In: Petrovský, E., Ivers, D., Harinarayana, T., Herrero-Bervera, E. (Eds.), The Earth's Magnetic Interior. Springer Netherlands, Dordrecht, pp. 361–397.
Orgeira, M.J., Walther, A.M., Tófalo, R.O., Vásquez, C., Berquó, T., Favier Dobois, C., Bohnel, H., 2003. Environmental magnetism in fluvial and loessic Holocene sediments and paleosols from the Chacopampean plain (Argentina). J. S. Am. Earth Sci. 16, 259–274. http://dx.doi.org/10.1016/S0895-9811(03)00067-1.
Orgeira, M.J., Walther, A.M., Vasquez, C.A., Tommaso, D.I., Alonso, S., Sherwood, G., Yuguan, H., Vilas, J.F.A., 1998. Mineral magnetic record of paleoclimate variation in loess and paleosol from the Buenos Aires formation (Buenos Aires, Argentina). J. S. Am. Earth Sci. 11, 561–570.
Özdemir, O., Dunlop, D.J., 2014. Hysteresis and coercivity of hematite. J. Geophys. Res. Solid Earth 119, 2582–2594. http://dx.doi.org/10.1002/2013JB010739.
Parry, L.G., 1982. Magnetization of immobilized particle dispersions with two distinct particle sizes. Phys. Earth Planet. In. 28, 230–241. http://dx.doi.org/10.1016/0031-9201(82)90004-8.
Pauthenet, R., 1950. Variation thermique de l'aimantation spontaneé des ferrites de nickel, cobalt, fer et manganese. Comptes Rendus de l'Académie des Sciences Series B 230, 1842–1844.
Peak, D., Regier, T., 2012a. Direct observation of tetrahedrally coordinated Fe(III) in ferrihydrite. Environ. Sci. Technol. 46, 3163–3168. http://dx.doi.org/10.1021/es203816x.
Peak, D., Regier, T.Z., 2012b. Response to comment on "Direct observation of tetrahedrally coordinated Fe(III) in ferrihydrite". Environ. Sci. Technol. 46, 6885–6887. http://dx.doi.org/10.1021/es302143n.
Peppe, D.J., Royer, D.L., Cariglino, B., Oliver, S.Y., Newman, S., Leight, E., Enikolopov, G., Fernandez-Burgos, M., Herrera, F., Adams, J.M., Correa, E., Currano, E.D., Erickson, J.M., Hinojosa, L.F., et al., 2011. Sensitivity of leaf size and shape to climate: global patterns and paleoclimatic applications. New Phytol. 190, 724–739. http://dx.doi.org/10.1111/j.1469-8137.2010.03615.x.
PiPujol, M.D., Buurman, P., 1997. Dynamics of iron and calcium carbonate redistribution and palaeohydrology in middle Eocene alluvial paleosols of the southeast Ebro Basin margin (Catalonia, northeast Spain). Palaeogeogr. Palaeoclimatol. Palaeoecol. 134, 87–107. http://dx.doi.org/10.1016/S0031-0182(97)00076-X.
Postma, D., 1983. Pyrite and siderite oxidation in swamp sediments. J. Soil Sci. 34, 163–182.
Porter, S.C., Hallet, B., Wu, X., An, Z., 2001. Dependence of near-surface magnetic susceptibility on dust accumulation rate and precipitation on the Chinese Loess Plateau. Quatern. Res. 55, 271–283. http://dx.doi.org/10.1006/qres.2001.2224.
Quinton, E.E., Dahms, D.E., Geiss, C.E., 2011. Magnetic analyses of soils from the Wind River Range, Wyoming, constrain rates and pathways of magnetic enhancement for soils from semiarid climates. Geochem. Geophys. Geosyst. 12 (Q07Z30). http://dx.doi.org/10.1029/2011GC003728.
Ranjard, L., Richaume, A., 2001. Quantitative and qualitative microscale distribution of bacteria in soil. Res. Microbiol. 152, 707–716.
Rankey, E.C., Farr, M.R., 1997. Preserved pedogenic mineral magnetic signature, pedogenesis, and paleoclimate change. Pennsylvanian Roca Shale (Virgilian, Asselian), central Kansas, USA. Sediment. Geol. 114, 11–32.
Retallack, G.J., 1991. Untangling the effects of burial alteration and ancient soil formation. Annu. Rev. Earth Planet. Sci. 19, 183–206.
Retallack, G.J., 2005. Pedogenic carbonate proxies for amount and seasonality of precipitation in paleosols. Geology 33, 333–336. http://dx.doi.org/10.1130/G21263.1.
Retallack, G.J., Sheldon, N.D., Cogoini, M., Elmore, R.D., 2003. Magnetic susceptibility of early Paleozoic and Precambrian paleosols. Palaeogeogr. Palaeoclimatol. Palaeoecol. 198, 373–380. http://dx.doi.org/10.1016/S0031-0182(03)00479-6.
Roberts, A.P., Liu, Q., Rowan, C.J., Chang, L., Carvallo, C., Torrent, J., Horng, C.S., 2006. Characterization of hematite (α-Fe2O3), goethite (α-FeOOH), greigite (Fe3S4), and

pyrrhotite (Fe7S8) using first-order reversal curve diagrams. J. Geophys. Res. Solid Earth 111, 1–16. http://dx.doi.org/10.1029/2006JB004715.
Robertson, D.J., France, D.E., 1994. Discrimination of remanence-carrying minerals in mixtures, using isothermal remanent magnetisation acquisition curves. Phys. Earth Planet. In. 82, 223–234. http://dx.doi.org/10.1016/0031-9201(94)90074-4.
Robinson, S.G., 1986. The late Pleistocene palaeoclimatic record of North Atlantic deep-sea sediments revealed by magnetic mineral measurements. Phys. Earth Planet. In. 42, 22–47. http://dx.doi.org/10.1016/S0031-9201(86)80006-1.
Rochette, P., Fillion, G., 1989. Field and temperature behavior of remanence in synthetic goethite: paleomagnetic implications. Geophys. Res. Lett. 16, 851–854. http://dx.doi.org/10.1029/GL016i008p00851.
Rochette, P., Mathé, P.E., Esteban, L., Rakoto, H., Bouchez, J.L., Liu, Q., Torrent, J., 2005. Non-saturation of the defect moment of goethite and fine-grained hematite up to 57 Teslas. Geophys. Res. Lett. 32, 1–4. http://dx.doi.org/10.1029/2005GL024196.
Roden, E.E., 2006. Geochemical and microbiological controls on dissimilatory iron reduction. Compt. Rendus Geosci. 338, 456–467. http://dx.doi.org/10.1016/j.crte.2006.04.009.
Royer, D., 2012. Climate reconstruction from leaf size and shape: new developments and challenges. In: Ivany, L.C., Huber, B.T. (Eds.), Reconstructing Earth's Deep-time Climate — The State of the Art in 2012. The Paleontological Society Papers 18, pp. 195–212.
Sangode, S.J., Bloemendal, J., 2004. Pedogenic transformation of magnetic minerals in Pliocene–Pleistocene palaeosols of the Siwalik Group, NW Himalaya, India. Palaeogeogr. Palaeoclimatol. Palaeoecol. 212, 95–118. http://dx.doi.org/10.1016/j.palaeo.2004.05.019.
Sangode, S.J., Kumaravel, V., Bloemendal, J., Kumar, R., 2008. Effect of burial and compaction on soil magnetic properties: results from soil–paleosol sequences in the Himalayan Foreland, India. Palaeogeogr. Palaeoclimatol. Palaeoecol. 267, 235–244. http://dx.doi.org/10.1016/j.palaeo.2008.06.020.
Schwertmann, U., 1988. Occurrence and formation of Iron oxides in various pedoenvironments. In: Stucki, J.W., Goodman, B.A., Schwertmann, U. (Eds.), Iron in Soils and Clay Minerals. Springer Netherlands, pp. 267–308.
Schwertmann, U., 1993. Relations between iron oxides, soil color, and soil formation. In: Bigham, J.M., Ciolkosz, E.J. (Eds.), Soil Color. Soil Science Society of America Publication 31, pp. 51–69. http://dx.doi.org/10.2136/sssaspecpub31.c4.
Schwertmann, U., Murad, E., 1983. Effect of pH on the formation of goethite and hematite from ferrihydrite. Clay Clay Miner. 31, 277–284.
Sharpe, J.L., 1996. Environmental archeology in central Alaska: A magneto-stratigraphic correlation of Tanana valley archeological sites with global climatic change. M.A. Thesis University of Minnesota, Minneapolis.
Sheldon, N.D., Retallack, G.J., 2001. Equation for compaction of paleosols due to burial. Geology 29, 247–250. http://dx.doi.org/10.1130/0091-7613(2001)029<0247.
Sheldon, N.D., Retallack, G.J., Tanaka, S., 2002. Geochemical climofunctions from North American soils and application to paleosols across the Eocene–Oligocene boundary in Oregon. Journal of Geology 110, 687–696.
Sheldon, N.D., Tabor, N.J., 2009. Quantitative paleoenvironmental and paleoclimatic reconstruction using paleosols. Earth Sci. Rev. 95, 1–52. http://dx.doi.org/10.1016/j.earscirev.2009.03.004.
Singer, M.J., Fine, P., Verosub, K.L., Chadwick, O.A., 1992. Time dependence of magnetic susceptibility of soil chronosequences on the California coast. Quatern. Res. 37, 323–332. http://dx.doi.org/10.1016/0033-5894(92)90070-Y.
Soreghan, G.S., Elmore, R.D., Katz, B., Cogoini, M., Banerjee, S., 1997. Pedogenically enhanced magnetic susceptibility variations preserved in Paleozoic loessite. Geology 25, 1003–1006. http://dx.doi.org/10.1130/0091-7613(1997)025<1003.
Soreghan, G.S.L., Elmore, R.D., Lewchuk, M.T., 2002. Sedimentologic-magnetic record of western Pangean climate in upper Paleozoic loessite (lower Cutler beds, Utah). Geol. Soc. Am. Bull. 114, 1019–1035. http://dx.doi.org/10.1130/0016-7606(2002)114<1019.
Sparks, N.H.C., Mann, S., Bazylinski, D.A., Lovley, D.R., Jannasch, H.W., Frankel, R.B., 1990. Structure and morphology of magnetite anaerobically-produced by a marine magnetotactic bacterium and a dissimilatory iron-reducing bacterium. Earth Planet. Sci. Lett. 98, 14–22.
Stacey, F.D., Banerjee, S.K., 1974. Developments in Solid Earth Geophysics, 5: The Physical Principles of Rock Magnetism. Elsevier Scientific Publishing Company, New York.
Stanjek, H., Fassbinder, J.W.E., Vali, H., Wägele, H., Graf, W., 1994. Evidence of biogenic greigite (ferrimagnetic Fe_3S_4) in soil. Eur. J. Soil Sci. 45, 97–103. http://dx.doi.org/10.1111/j.1365-2389.1994.tb00490.x.
Stinchcomb, G.E., Peppe, D.J., 2014. The influence of time on the magnetic properties of late Quaternary periglacial and alluvial surface and buried soils along the Delaware River, USA. Front. Earth Sci. 2, 1–14. http://dx.doi.org/10.3389/feart.2014.00017.
Stober, J.C., Thompson, R., 1979. An investigation into the source of magnetic minerals in some Finnish lake sediments. Earth Planet. Sci. Lett. 45, 464–474. http://dx.doi.org/10.1029/91JB03068.
Stockhausen, H., 1998. Some new aspects for the modelling of isothermal remanent magnetization acquisition curves by cumulative log Gaussian functions. Geophys. Res. Lett. 25, 2217–2220.
Tauxe, L., Banerjee, S.K., Butler, R.F., van der Voo, R., 2014. Essentials of Paleomagnetism. University of California Press.
Taylor, R.M., Maher, B.A., Self, P.G., 1987. Magnetite in soils: I. The synthesis of single-domain and superparamagnetic magnetite. Clay Miner. 22, 411–422.
Thompson, R., Maher, B.A., 1995. Age models, sediment fluxes and paleoclimatic reconstructions for the Chinese loess and palaeosol sequences. Geophys. J. Int. 123, 611–622.
Thompson, R., Oldfield, F., 1986. Environmental Magnetism. Springer.
Till, J.L., Guyodo, Y., Lagroix, F., Morin, G., 2015. Goethite as a potential source of magnetic nanoparticles in sediments. 43, 75–78. http://dx.doi.org/10.1130/G36186.1.
Till, J.L., Guyodo, Y., Lagroix, F., Ona-Nguema, G., Brest, J., 2014. Magnetic comparison of abiogenic and biogenic alteration products of lepidocrocite. Earth Planet. Sci. Lett. 395, 149–158. http://dx.doi.org/10.1016/j.epsl.2014.03.051.
Tohver, E., Weil, A.B., Solum, J.G., Hall, C.M., 2008. Direct dating of carbonate remagnetization by 40Ar/39Ar analysis of the smectite–illite transformation. Earth Planet. Sci. Lett. 274, 524–530. http://dx.doi.org/10.1016/j.epsl.2008.08.002.
Torrent, J., Barrón, V., Liu, Q., 2006. Magnetic enhancement is linked to and precedes hematite formation in aerobic soil. Geophys. Res. Lett. 33, L02401. http://dx.doi.org/10.1029/2005GL024818.
Torrent, J., Liu, Q.S., Barrón, V., 2010a. Magnetic minerals in Calcic Luvisols (Chromic) developed in a warm Mediterranean region of Spain: origin and paleoenvironmental significance. Geoderma 154, 465–472. http://dx.doi.org/10.1016/j.geoderma.2008.06.020.
Torrent, J., Liu, Q.S., Barrón, V., 2010b. Magnetic susceptibility changes in relation to pedogenesis in a Xeralf chronosequence in northwestern Spain. Eur. J. Soil Sci. 61, 161–173. http://dx.doi.org/10.1111/j.1365-2389.2009.01216.x.
Torrent, J., Liu, Q.-S., Bloemendal, J., Barron, V., 2007. Magnetic enhancement and iron oxides in the upper Luochuan loess–paleosol Sequence, Chinese Loess Plateau. 71. http://dx.doi.org/10.2136/sssaj2006.0328.
Tramp, K.L., Soreghan, G.S., Elmore, R.D., 2004. Paleoclimatic inferences from paleopedology and magnetism of the Permian Maroon Formation loessite, Colorado, USA. Geol. Soc. Am. Bull. 116, 671. http://dx.doi.org/10.1130/B25354.1.
van Velzen, A.J., Dekkers, M.J., 1999. Low-temperature oxidation of magnetite in loess–paleosol sequences: a correction of rock magnetic parameters. Stud. Geophys. Geod. 43, 357–375. http://dx.doi.org/10.1023/A:1023278901491.
Vidic, N.J., Singer, M.J., Verosub, K.L., 2004. Duration dependence of magnetic susceptibility enhancement in the Chinese loess–palaeosols of the past 620 ky. Palaeogeogr. Palaeoclimatol. Palaeoecol. 211, 271–288. http://dx.doi.org/10.1016/j.palaeo.2004.05.012.
Weiss, J.V., Emerson, D., Megonigal, J.P., 2004. Geochemical control of microbial Fe(III) reduction potential in wetlands: comparison of the rhizosphere to non-rhizosphere soil. FEMS Microbiol. Ecol. 48, 89–100. http://dx.doi.org/10.1016/j.femsec.2003.12.014.
Woods, S.D., Elmore, R.D., and Engel, M.H., 2002. Paleomagnetic dating of the smectite-to-illite conversion: testing the hypothesis in Jurassic sedimentary rocks, Skye, Scotland. J. Geophys. Res., v. 107, B5 2091, doi: http://dx.doi.org/10.1029/2000JB000053.
Worm, H.U., Markert, H., 1987. The preparation of dispersed titanomagnetite particles by glass–ceramic method. Phys. Earth Planet. In. 46, 263–269.
Yamazaki, T., Ioka, N., 1997. Environmental rock magnetism of pelagic clay: implications for Asian eolian input to the North Pacific since the Pliocene. Paleoceanography 12, 111–124. http://dx.doi.org/10.1029/96PA02757.
Zhang, Y.G., Ji, J., Balsam, W.L., Liu, L., Chen, J., 2007. High resolution hematite and goethite records from ODP 1143, South China Sea: co-evolution of monsoonal precipitation and El Nino over the past 600,000 years. Earth Planet. Sci. Lett. 264, 136–150. http://dx.doi.org/10.1016/j.epsl.2007.09.022.